Use of ion clustering equilibrium for isomer identification in electron capture mass spectrometry
by Lisa A Krieger

A thesis submitted in partial fulfillment of the requirements for the degree of Master of Science in Chemistry
Montana State University

Abstract:
This work explores the possibility of isomer distinction by taking advantage of unique solvation equilibrium constants for the clustering of ions with neutral solvating molecules. Each isomer would exhibit a unique ratio of MS-/M- from a mass spectrum of the compound and the solvating molecule which could theoretically be predicted if the equilibrium constant and the solvating molecule concentration are known. This is assuming that equilibrium exists in the source, which is shown to be true for the atmospheric pressure ionization source.

A number of substituted nitrobenzenes were tested with dimethylsulfoxide (DMSO) as the neutral solvating molecule. These experiments showed that the method has promise, but is not as straightforward as the theory predicts. An attempt was made to mathematically describe the observed deviations from expectation. This resulted in an expression that closely described the system, but could not calculate the reference value of Kf.

USE OF ION CLUSTERING EQUILIBRIUM FOR ISOMER IDENTIFICATION IN ELECTRON CAPTURE MASS SPECTROMETRY

by

Lisa A. Krieger

A thesis submitted in partial fulfillment
of the requirements for the degree

of

Master of Science

in

Chemistry

MONTANA STATE UNIVERSITY
Bozeman, Montana

March 1987

APPROVAL

of a thesis submitted by

Lisa A. Krieger

This thesis has been read by each member of the thesis committee and has been found to be satisfactory regarding content, English usage, format, citations, bibliographic style, and consistency, and is ready for submission to the College of Graduate Studies.

3/6/87
Date

Eric Grimsrud
Chairperson, Graduate Committee

Approved for the Major Department

3/6/87
Date

Head, Major Department

Approved for the College of Graduate Studies

March 9, 1987
Date

Henry L Parsons
Graduate Dean

STATEMENT OF PERMISSION TO USE

In presenting this thesis in partial fulfillment of the requirement's for a master's degree at Montana State University, I agree that the Library shall make it available to borrowers under rules of the Library. Brief quotations from this thesis are allowable without special permission, provided that accurate acknowledgement of source is made.

Permission for extensive quotation from or reproduction of this thesis may be granted by my major professor, or in his/her absence, by the Director of Libraries when, in the opinion of either, the proposed use of the material is for scholarly purposes. Any copying or use of the material in this thesis for financial gain shall not be allowed without my written permission.

Signature Lisa A. Krieger

Date March 6, 1987

TABLE OF CONTENTS

LIST OF TABLES

LIST OF FIGURES

ABSTRACT

This work explores the possibility of isomer distinction by taking advantage of unique solvation equilibrium constants for the clustering of ions with neutral solvating molecules. Each isomer would exhibit a unique ratio of MS^-/M^- from a mass spectrum of the compound and the solvating molecule which could theoretically be predicted if the equilibrium constant and the solvating molecule concentration are known. This is assuming that equilibrium exists in the source, which is shown to be true for the atmospheric pressure ionization source.

A number of substituted nitrobenzenes were tested with dimethylsulfoxide (DMSO) as the neutral solvating molecule. These experiments showed that the method has promise, but is not as straightforward as the theory predicts. An attempt was made to mathematically describe the observed deviations from expectation. This resulted in an expression that closely described the system, but could not calculate the reference value of K_f.

INTRODUCTION

One of the most sensitive detection techniques for trace analysis is electron-capture mass spectrometry (ECMS). There are two routes the electron-capture process can take. One is resonance electron capture, where a thermalized electron is captured by a molecule to form the molecular anion, as shown by route 1a below. The other is dissociative electron capture, as shown by route 1b, which involves the dissociation of the molecular anion as it captures the electron.

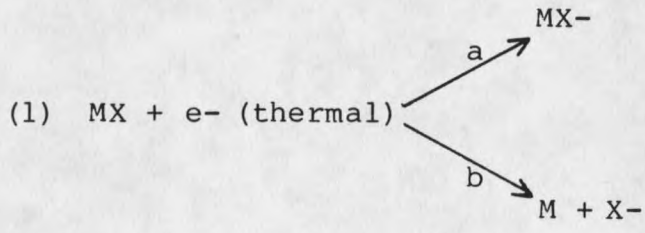

ECMS is a sensitive technique compared to other ionization reactions because electron-capture is one of the fastest ionic reactions, having a rate constant, k_{ec}, up to 4×10^{-7} cm^3/sec. Ion-molecule reactions are no faster than $k_{i/m} = 1 \times 10^{-9}$ cm^3/sec, which is two orders of magnitude slower than electron capture. The speed of reaction is one reason for ECMS sensitivity. The other reason is that in the resonance EC process the analyte forms the molecular ion, M^-, with little or no fragmentation. Thus, identification and quantitation can be monitored from the same signal. With only M^- being formed, trace

amounts are detectable since the total available signal is concentrated on one ion, M^-. The one problem with ECMS is that although it provides sensitive signals for trace analysis, it often does not indicate which isomer is present. Since isomers differ only in the physical orientation of the atoms in the molecule, the masses of two or more isomers are identical, thus it is impossible to distinguish between them with electron-capture mass spectrometry if the signal is M^-.

Kebarle and co-workers have been studying the solvation of molecular anions by neutral molecules such as dimethylsulfoxide, acetonitrile, and methanol.[1] The molecular ion, M^-, is solvated by the neutral solvator, S, to form a cluster ion, MS^-. This reaction requires a buffer gas, B, to collisionally stabilize the cluster ion so it does not immediately fall apart. The reverse of reaction 2 also occurs.

$$(2) \quad M^- + S \longrightarrow MS^{-*} \xrightarrow{B} MS^-$$

The equilibrium expression for the solvation of M^- by S is:

$$(3) \quad K_f = \frac{[MS^-]}{[M^-][S]}$$

and then:

$$(4) \quad K_f[S] = \frac{[MS^-]}{[M^-]} \ .$$

According to Kebarle,[1] the K_f values vary between isomers for substituted nitrobenzenes (NB). Table 1 shows some of these compounds and their respective K_f values for the solvating compounds, methanol, acetonitrile and dimethylsulfoxide.

Table 1. K_f[K] Values for Compounds at 70°C

	K_f		
Compound	CH_3OH	CH_3CN	DMSO
o-FNB	5.1×10^3		
m-FNB	3.6×10^3	6.5×10^3	9.8×10^4
p-FNB	7.0×10^3	1.0×10^4	1.6×10^5
o-diNB	1.3×10^2	1.2×10^3	8.9×10^3
m-diNB	2.5×10^2	5.2×10^2	5.3×10^3
p-diNB	3.0×10^1	1.0×10^2	6.6×10^2

Since K_f is dependent upon isomeric differences of a given compound, the value $[MS^-]/[M^-]$ should change with the isomer in accordance with equation 4. This solvation equilibrium could then be applied to analytical mass spectrometry assuming five conditions:

1. The equilibrium constants of the isomers must not be equal, ie. $K_{ortho} \neq K_{meta} \neq K_{para}$
2. S, the solvating molecule, must not capture electrons.
3. S must be a good solvator of negative ions so that MS^- as well as M^- is observable.
4. The system must be in equilibrium so that $K_f[S] = [MS^-]/[M^-] = \text{CONSTANT}$.
5. The mass spectrometer must accurately measure $[MS^-]/[M^-]$.

Condition #1 has been shown to be true for substituted nitrobenzenes as described previously. Conditions #2 and #3 are met by choosing an appropriate solvent, molecule such as dimethylsulfoxide (DMSO), that has a sufficiently large K_f value with the analyte of interest to give observable signals for both M^- and MS^-. It also must not give a significant background spectrum. Condition #4 states that the system must be in equilibrium. Whether or not this is true will depend on what type of ionization system is chosen to work with. Two possible choices are negative chemical ionization (NCI) and atmospheric pressure ionization (API). By analyzing the chemical dynamics of the reactions in both systems, one of these turns out to be the more likely system in which the solvating equilibrium will take place.

Condition #5 requires that the mass spectrometer accurately measures the ratio, R, of $[MS^-]/[M^-]$ in the source. This condition may be difficult to meet, as the transport of ions through the aperture into the mass analyzing region may be accompanied by collisions which could dissociate MS^-.[2] In the APIMS extreme pressure and temperature gradients exist in the region of the aperture which may also alter the observed R from the actual value of R that is in the source.

STATEMENT OF THE PROBLEM

As shown in the introduction, the identification of isomers may be possible using a neutral solvating molecule. Each isomer should have a characteristic ratio of $[MS^-]/[M^-]$, stemming from a different K_f value.

The purpose of this research is to explore the method described in the introduction to see if the solvation equilibria method works and the theory holds under conditions of analysis by GC/ECMS. The equilibrium between two ions will be examined and compared to expected values to determine if equilibrium is achieved. If there are any deviations from the theory, an attempt will be made to explain them.

CHEMICAL DYNAMICS

The fourth condition necessary for distinguishing isomers by solvation equilibria, that of requiring equilibrium, can be theoretically examined by predicting the chemical dynamics in the ion source. The equations obtained from these predictions should reduce to $K_f[S] = [MS^-]/[M^-]$, if equilibrium is achieved in the source.

The ion and electron reactions in NCI and API are similar as shown in reactions 5 - 12 below. The identities of some species such as B and P^+ may differ between API and NCI, but the reactions as written occur for both methods. A more detailed description of how the NCI ionization source works is given by Harrison.[3] The API source is described by McKeown and Siegel.[4] The following reactions describe what is happening within either source. P^+ means any positive ion, the rate constant, F/V, is the volumetric flow rate through the source divided by the volume of the source, and the diffusion constant, D/r_o^2, is a value that is dependent on the geometry of the source. This rate constant will be given a numerical value later. All of the rate constants have been chosen to present the most favorable case.

Formation Reactions

(5) $M + e^- \longrightarrow M^-$ $\quad k_{ec} = 4 \times 10^{-7}$ cc/sec [5]

(6) $M^- + S + B \longrightarrow MS^- + B$ $\quad k_{sol} = 1 \times 10^{-27}$ cc^3/sec

Loss Reactions

(7) $MS^- + B \longrightarrow M^- + S + B$

(8) $M^- + P^+ \longrightarrow$ NEUTRALS

(9) $MS^- + P^+ \longrightarrow$ NEUTRALS $\quad R_i$ depends on pressure[5]

(10) $e^- + P^+ \longrightarrow$ NEUTRALS $\quad R_{e-} = 8 \times 10^{-7}$ cc/sec [5]

(11) ALL ions, radicals, neutrals $\longrightarrow$ VENT $\quad k = F/V$

(12) ALL ions, etc. $\longrightarrow$ DIFFUSION TO WALLS $\quad k = D/r_o^2$

From the above equations, an expression can be written for the production of MS^- with time:

$$(13) \quad d[MS^-]/dt = k_{sol}[M^-][S][B] - k_{-sol}[MS^-][B] - R_i[MS^-][P^+] - [F/V][MS^-] - [D/r_o^2][MS^-]$$

The steady state approximation, $d[MS^-]/dt = 0$, may be applied to this flow-through reactor in which mixing by diffusion is much more rapid than ventilation through the cell. Setting equation 13 equal to zero and rearranging, results in equation 14:

$$(14) \quad \frac{[MS^-]}{[M^-]} = \frac{k_{sol}[S][B]}{k_{-sol}[B] + R_i[P^+] + F/V + D/r_o^2}$$

Condition four states:

$$(15) \quad \frac{[MS^-]}{[M^-]} = K_f[S]$$

Equation 14 can reduce to equation 15 only if the last three terms in the denominator, $R[P^+] + F/V + D/r_o^2$, are negligible with respect to the first term, $k_{-sol}[B]$.

Using the following typical NCI values for the parameters in the denominator of equation 14:

$k_{sol} = 1 \times 10^{-27}$ cc/sec

$[S] = 2 \times 10^{15}$ cc^{-1} (at 0.1 Torr)

$[B] = 2 \times 10^{16}$ cc^{-1} (at 1 Torr)

$R_i = 6.4 \times 10^{-8}$ cc/sec [6]

$[P^+] = 3 \times 10^{10}$ cc^{-1}

$F/V = 100$ sec^{-1} (100cc/sec/cc)

$D = 100$ cm^2/sec (at 1 Torr) [5]

$r_o^2 = 0.02$ cm^2 [5]

$k_{-sol} = 1.7 \times 10^{-12}$ cc/sec

(The value for k_{-sol} was calculated from Eq. 14 using the above values and assuming an observable ratio of 1.)

From the values given:

$k_{-sol}[B] = 3.4 \times 10^4$

$R[P^+] + F/V + D/r_o^2 = 7.0 \times 10^3$.

The sum of the last three terms of the denominator, which are due to recombination, ventilation, and diffusion respectively, is about 20 percent of the first term, so negligibility is not proved.

Using the maximum value for [S] under NCI conditions (1.3×10^{-4} atm.), and assuming a reasonable K_f value (500 $atm.^{-1}$), the maximum theoretical ratio is obtained from equation 15:

$$[MS^-]/[M^-] = K_f[S] = (500 atm.^{-1})(1.3 \times 10^{-4} atm.) = 0.065$$

This maximum signal for MS^- is less than 1 percent that of M^-, which would make MS^- difficult to observe. Since [S] cannot be further increased to favor formation of MS^-, NCI is not a favorable ionization technique for this type of isomer distinction.

The following values for API can be applied in the same manner. k_{-sol} has been calculated the same way as before.

$k_{-sol} = 7 \times 10^{-11}$ cc/sec

$k_{sol} = 1 \times 10^{-27}$ cc^2/sec

$[B] = 1 \times 10^{19}$ cc^{-1}

$[S] = 7 \times 10^{16}$ cc^{-1}

$R_i = 1 \times 10^{-6}$ cc/sec [5]

$[P^+] = 10^8$ cc^{-1}

$F/V = 1$ sec^{-1} (1 cc/sec/1 cc)

$D = 0.25$ cm^2/sec [7]

$r_o^2 = 0.04$ cm^2 [7]

From the API values:

$$k_{-sol}[B] = 7 \times 10^8$$

$$R_i[P^+] + F/V + D/r_o^2 = 107.25$$

The last three terms in the denominator are definitely negligible with respect to the first term. This enables the complete expression for R to reduce to equation 15, $[MS^-]/[M^-] = K_f[S]$, which suggests that the solvation equilibria method of isomer distinction in the API is theoretically possible.

The reason API is predicted to surpass NCI for this type of analysis lies in the fact that the solvation reaction is third order. The rate of a third order reaction is calculated by:

$$(16) \quad \text{Rate} = k_{sol}[M^-][S][B].$$

Since the buffer gas concentration is close to three orders of magnitude higher in API than NCI, the rate of reaction is much faster in API. This rate is $7 \times 10^8[M^-]$ compared to the NCI rate of $4 \times 10^4[M^-]$. Also, the concentration of the solvating molecule can be made higher in API, further increasing the rate of the solvating reaction.

Using an easily achieved value of [S], 5×10^{-3}atm., and a K_f of 500, the calculated R would be 2.5. This would provide an easily observable ratio of signals. Thus, according to theory under reasonable operating conditions, the API source should work for this method of isomer distinction.

EXPERIMENTAL

The instrument used in this research was a specialized, home-built mass spectrometer. The source was an atmospheric pressure ionization source that could also be used as an ECD or a corona discharge source. A detailed description of the source will be given later. To introduce samples into the source, a gas chromatograph was used with nitrogen as the carrier gas. The nitrogen was passed through oxygen and water-removing traps prior to entering the column.

The gas chromatograph was a Gow-Mac model 750 that was modified to accommodate a Hewlett Packard 530 micrometer, 10 meter macrobore column (number 19095Z-121). The macrobore column was installed to reduce the amount of column bleed introduced into the source. The column was threaded through a stainless steel, heated, transfer line and fed directly into the source. The net result was that the column ended approximately flush with the entrance into the source.

Two methods were used to introduce the solvent molecules into the source. The first one was via a diluter, which was a large, airtight volume, with make-up gas flowing through it and into the source to mix with the GC effluent. The dilution volume has a septum port which allows the injection of a known quantity of solvating compound into the diluter. This is then diluted by the make-up gas and some is carried into the source. Knowing the

flow rate through the diluter, the total flow rate through the source, the volume of the diluter, the pressure inside the diluter (which in most cases is atmospheric), the amount of solvating molecule injected, and the time from the initial injection, the concentration of the solvating molecules in the source can be calculated. The amount flowing out of the diluter at any time can be calculated from: $C = C_o e^{-(F/V)t}$, where F is the volumetric flow rate through the diluter, V is the volume of the diluter and t is the time elapsed since injection of the solvating molecule. Once C is found, the amount of solvating molecule in the source is: $C_s = C(F_d/F_t)$, where F_d is the flow rate through the diluter and F_t is the total flow rate of both the column and the make-up gas through the source.

A disadvantage of this system is that the concentration of S, the solvating compound, is always changing due to the constant flow of make-up gas into and out of the diluter. Also, it takes days to completely clean the diluter of one solvator in preparation for a different one. Another problem is that the choice of solvating compounds is limited because they have to have sufficient vapor pressure to evaporate into the diluter. Another system was devised to alleviate these drawbacks of the diluter.

The second system tested was called a "bubbler". The first of these constructed was a simple cylindrical tube, one inch in diameter, with a one-quarter inch glass tube that was drawn to a fine opening inside the larger cylinder. This was the make-up

gas inlet. With the bubbler filled with a sufficient amount of solvating compound, nitrogen was bubbled through the liquid to saturate the gas with the solvating liquid. The saturated gas was then allowed out via a glass exit port in the side, near the top of the large cylinder. See Figure 1.

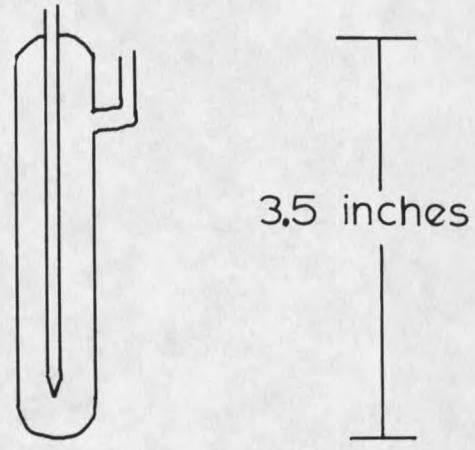

Figure 1. First Bubbler.

With the above design, there was some question as to the efficiency of saturation of the make-up gas. Another bubbler was designed to eliminate this possible problem. The basic design is shown in Figure 2.

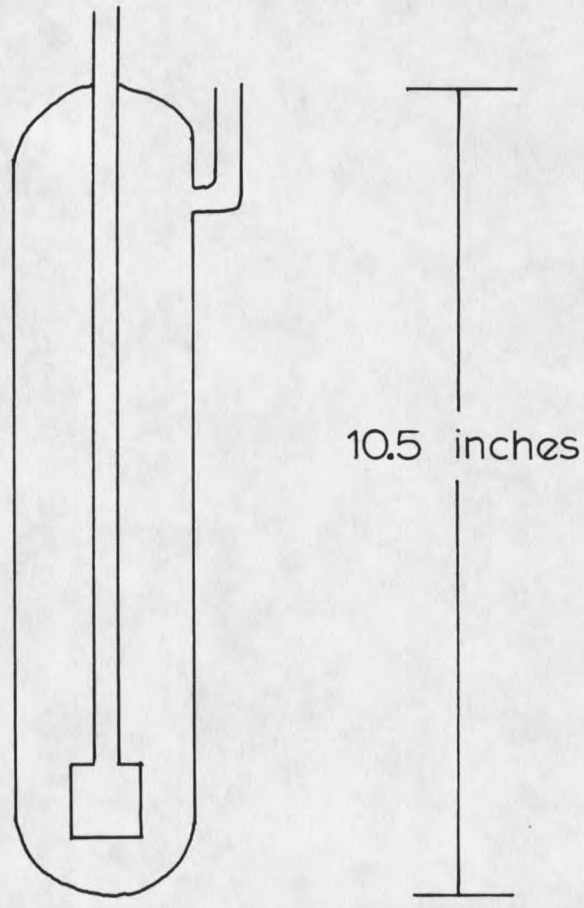

Figure 2. Second Bubbler.

The differences are changes in dimension and the use of an LC column end which has a sintered glass frit on the end. The sintered glass forms smaller bubbles than the original design. These smaller bubbles are more easily saturated than those produced in the original design. The dimensions were increased to a diameter of one and one half inches to accommodate the

larger bubbler tube. The height was also increased so the vertical distance traversed by the bubbles was longer, increasing the chance of saturating the bubbles. With an increase in the dimensions comes the increase of volume. This larger volume results in a larger solvent capacity, enabling a longer use as the bubbler will need to be refilled less often. As will be shown later, the two different designs of bubblers made no difference in the results. Therefore, saturation of the nitrogen gas appeared to be achieved in both cases.

Once the analyte and the solvator molecules are in their respective gas lines, they are combined in the source of the API. The source is a homemade electron capture detector (ECD) which consists of a volume of about 1 cm^3 with a gas inlet and outlet, and is bolted onto the front of the vacuum envelope of the quadrupoles as shown in Figure 3. This volume is lined with a platinum cylinder imbedded with 9 mCi of nickel 63. The aperture of the source leading to the vacuum envelope and mass analyzer is in a 5/8 inch diameter disk of nickel, which is 25 microns thick. The aperture is 20 microns in diameter. There is also a stainless steel pin mounted coaxially in the source which can serve as a corona discharge or as the anode of an ECD.

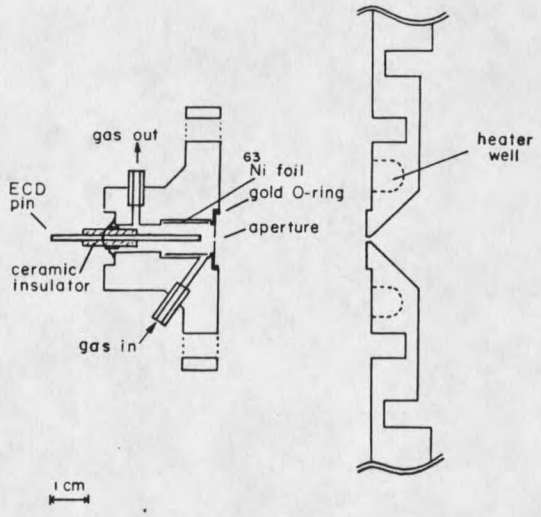

Figure 3. ECD Source of Mass Spectrometer with Front Flange of Vacuum Envelope.

The mass analyzer itself is a quadrupole design by Extra-Nuclear, Model 162-8, capable of better than unit mass resolution up to a mass of 500. The detector is a channeltron 4039 electron multiplier by Galileo Electro-Optics. The analog signal from a ratemeter (Ortec Model 441) is recorded by a chart recorder. Figure 4 shows a block diagram of the setup.

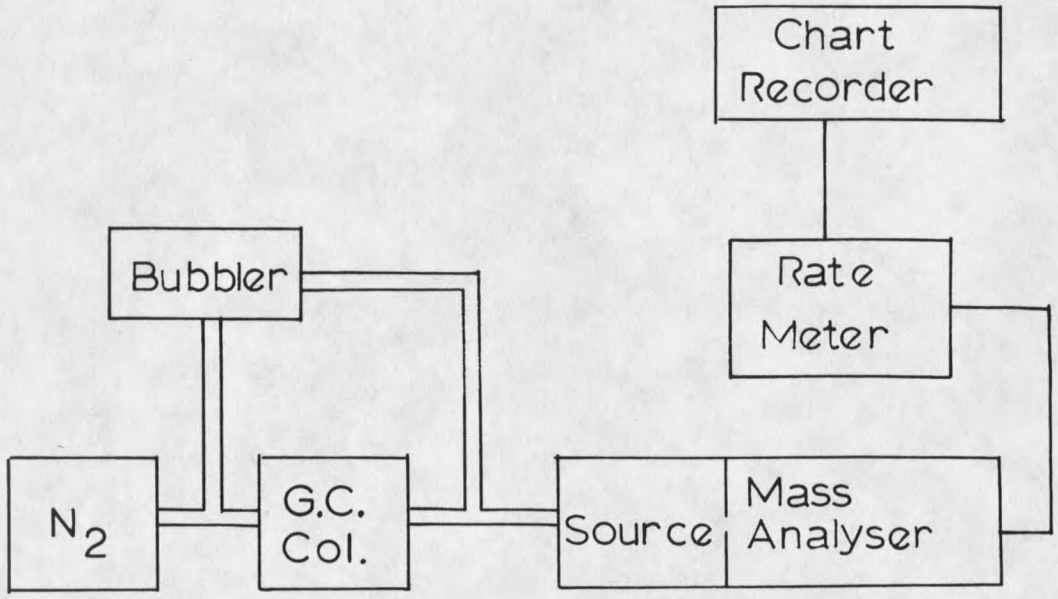

Figure 4. Block Diagram of Instrument.

This mass spectrometer can perform mass spectra scans, single and total ion monitoring, and one more function that was developed especially for this project. This latter function is the dual ion monitor, or DIM. This was necessary in order to monitor two different ions as one compound elutes from the G.C. column. Once every time interval, such as one second, the mass analyzer selects first one, and then the other ion and sends the signal to the recorder. The net result is a printout that looks like Figure 5. The circuit was made with the following integrated circuits: 3140 op amps and an integrated circuit switch AD7512DKN. The other components were two manual switches,

a small, red light, and various resistors, variable resistors and capacitors. Figure 6 shows the resulting circuit.

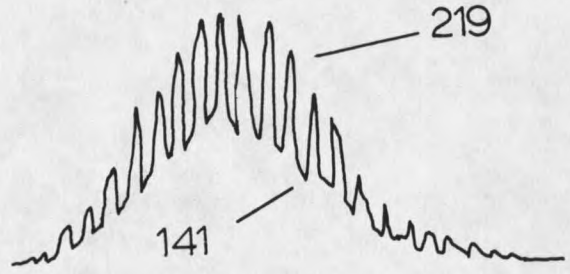

Figure 5. Sample of DIM Printout.

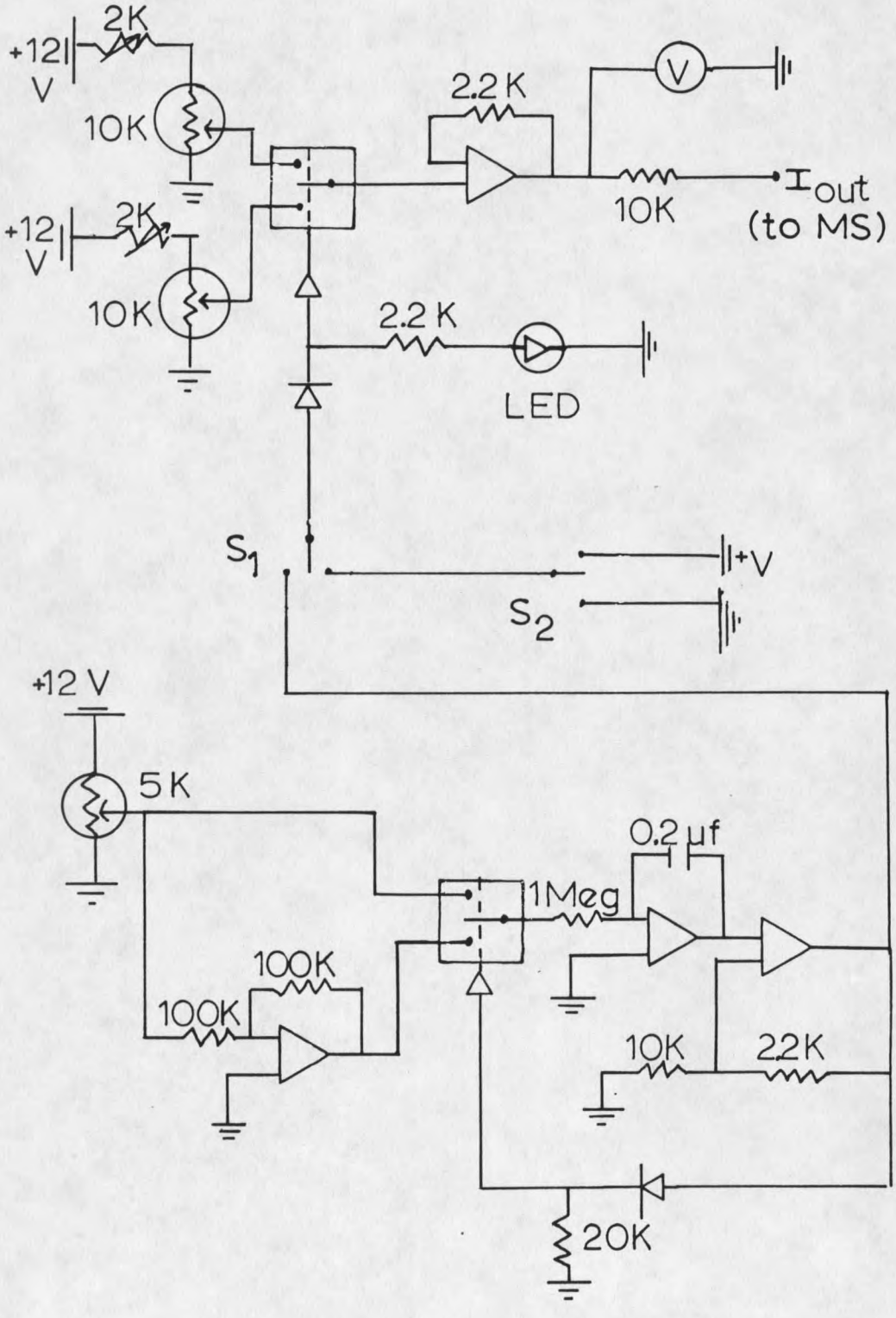

Figure 6. DIM Circuit.

The compounds used were para-cyanonitrobenzene (p-CNNB), ortho-, meta-, and para-fluoronitrobenzene (o, m, and p-FNB), meta and para-nitroanisole (m and p-OCH_3NB), m-trifluoronitrotoluene (m-CF_3NB), ortho-, meta-, and para-dinitrobenzene (o, m, and p-diNB), and ortho-, meta-, and para-nitrotoluene (o, m, and p-NT). The analytes were obtained from Aldrich Chemical in 99^+% purity. No further purification was done on the analytes. The solvating molecule, dimethylsulfoxide (DMSO), came from Baker and was distilled prior to use. The one solvent, benzene, was reagent grade from Baker. This was not further purified.

The samples used were made up in benzene to a concentration of 5 to 30 ng/microliter. Gaseous samples were injected directly into a diluter, used in place of the column, and allowed to flow into the source with the carrier gas. Once the samples were introduced into the source, both the M^- and MS^- ions were monitored.

To determine the K_f values of the solvating reactions, and to see if equilibrium is indeed achieved in the API source, various sets of data were collected. Monitoring M^-, MS^- and knowing the concentration of S, the experimental value of K_f can be calculated.

Data was collected for plots of K_f vs. [S] and various other manipulations of that data such as 1/K vs. [S], ln K vs. [S], and 1/R vs. 1/[S]. The reason the K_f vs. [S] data was collected was

to check the constancy of K_f over various concentrations of the solvator.

The S concentration was varied by raising the temperature of a water bath containing the bubbler via a hot plate. A foil lid was secured over the top of the bath around the inlets and outlets to the bubbler to keep the heat in and reduce evaporation of the water bath. Heating tape was coiled around the gas line leaving the bubbler, and wrapped all the way along it to the source. Care was taken to keep this gas line at a higher temperature than the water bath to prevent condensation of the solvating molecule in the line. With this set-up, the concentration of S can be calculated to a fairly reliable value, and easily controlled.

The monitoring of M^- and MS^- completes the experiment. Several different methods of monitoring M^-, MS^- and R were used, first scanning, then single ion monitoring (SIM), and finally dual ion monitoring (DIM).

CALCULATION OF EXPECTED K_f VALUES

The original instrument used a diluter in the make-up gas line to deliver the solvating molecule to the source, and a column was used to introduce the analyte. With this set-up, preliminary data was retrieved to see if this project was worth pursuing. The two solvating compounds checked were DMSO and methanol. These were chosen because there are known K_f values for these compounds with various substituted benzenes such as the fluoronitrobenzenes, nitrotoluenes, nitroanilines and others.[1]

The known K_f values were all obtained at 70°C. Unfortunately, the compounds used require a column temperature of around 70°C, so the solvating data from this set-up must be taken at 125°C or higher. This is because the source must be kept at least 50° higher than the incoming gas. In order to compare the experimental K_f values at 150°C, to K_f^K at 150°, the Kebarle K_f^{150} values must be calculated from the 70 degree data using the given ΔH and ΔS values, as shown below:

$$\Delta G = -RT\ln K_f$$

$$\Delta G = \Delta H - T\Delta S$$

For example, to find K_f at 150° for the solvation of m-CF_3NB with DMSO:

ΔG^{70} = -7.1 kcal/mole, ΔH^{70} = -14.6 kcal/mole,

ΔS^{70} = -22.3 cal/mole

$150^{o}C = 423^{o}K$

$\Delta G^{423} = -14.6 - (423)(-0.0223)$

ΔG^{423} = -5.167 kcal/mole

$\Delta G^{423} = -RT\ln K$

$-5.167 = -(1.987 \times 10^{-3})(423)\ln K$

$K_f{}^{K} = 467.5$ atm.$^{-1}$

According to Kebarle, there are errors in his measurements for ΔH and ΔS,[1] thus the K^{150} can be approximated to 500 atm.$^{-1}$. All known K_f values used for comparison were calculated up to an experimental temperature of 150°C by this method. They are listed in Table 2.

Table 2. Calculated Values of $K_f{}^{150}$

Compound	ΔH kcal/mole	ΔS cal/mole-deg	K_f atm.$^{-1}$
p-OCH_3NB	-16.3	-22.5	320
m-CF_3NB	-14.6	-22.3	468
p-CNNB	-16.0	-33.6	8

Once the K_f values are found, the ratio, R, of the Intensity MS^-/Intensity M^- can be predicted. This comes directly from the equilibrium expression,

$$K_f = \frac{[MS^-]}{[M^-][S]}$$

where:

$$R = \frac{[MS^-]}{[M^-]}$$

and

$$K_f[S] = R$$

Thus, knowing K_f and [S], R may be predicted.

RESULTS

With the original diluter, to find [S], the temperature of the room must be known in order to get the vapor pressure of the solvent. Then the appropriate volume of solvent molecule can be injected so as not to leave any liquid unevaporated. For example, at 20°C the vapor pressure of DMSO is 5×10^{-4} atm. The volume of the diluter is 6 liters and is at atmospheric pressure. To get the initial concentration of S, start with the ideal gas law and rearrange to equation 20:

$$(20) \quad \frac{PV}{RT} = n$$

$$\frac{(5 \times 10^{-4})(6L)}{(0.0821)(293)} = n = 1.25 \times 10^{-4} \text{ moles}$$

$$(1.25 \times 10^{-4} \text{moles})(78\text{g/mole})(1\text{cc}/1.1014\text{g}) =$$

$$= 8.83 \times 10^{-3} \text{ cc}$$

Injecting 8.83 microliters of DMSO would give the maximum concentration possible at 20°C, 0.38 torr (5×10^{-4} atm. = 0.38 torr).

Preliminary experiments, done with the diluter to introduce the solvator, showed that solvation does indeed occur in the API source, and is observable as shown in Figures 7 - 11. As can be seen from these Figures, there is a definite difference between the background ions when either MeOH or DMSO is present. MeOH

tends to give a lot of background ions with no analyte present, and extraneous ions when the analyte passes through the source. See Figures 9 - 12. DMSO gives comparatively little background ions, and no extraneous ions during the solvation. Thus, for the purposes of this research, DMSO is the better solvator and is the only compound that will be used in that capacity.

An experiment was run on the NCIMS to check the assumption that it would not facilitate solvation for isomer identification. The results showed that no solvation occurred for nitrobenzene. The partial pressure of methanol, the solvator, was 10% of the total ion source pressure. In API experiments, significant solvation takes place with the partial pressure of methanol much less than 1% of the total ion source pressure.

Since solvation of M^- occurs in the API, the ratio, $R = [MS^-]/[M^-]$, can be measured and compared to the calculated, expected R that is predicted to be a constant value. Table 3 shows the values for R and the intensities of the M^- and MS^- ions, 191 and 269 mass units, for the system of m-CF_3NB and DMSO. The predicted R for this experiment is 0.26, reasonably close to the first scan, but significantly different for the other scans. For a value that is predicted to be constant, R appears to change drastically.

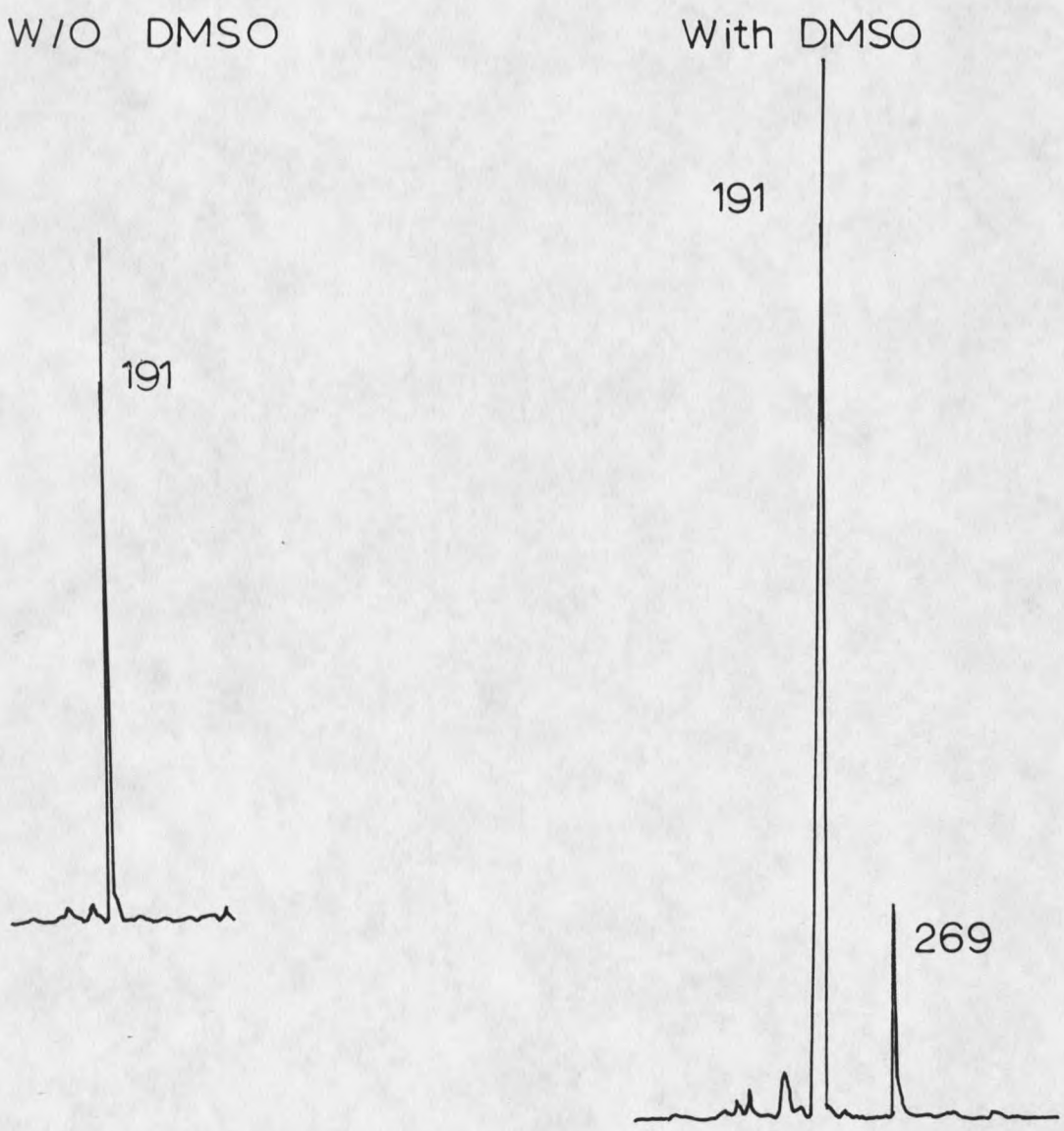

Figure 7. Ion scan of m-CF_3NB and DMSO. 269 is the solvated molecular ion, 191 is the molecular ion.

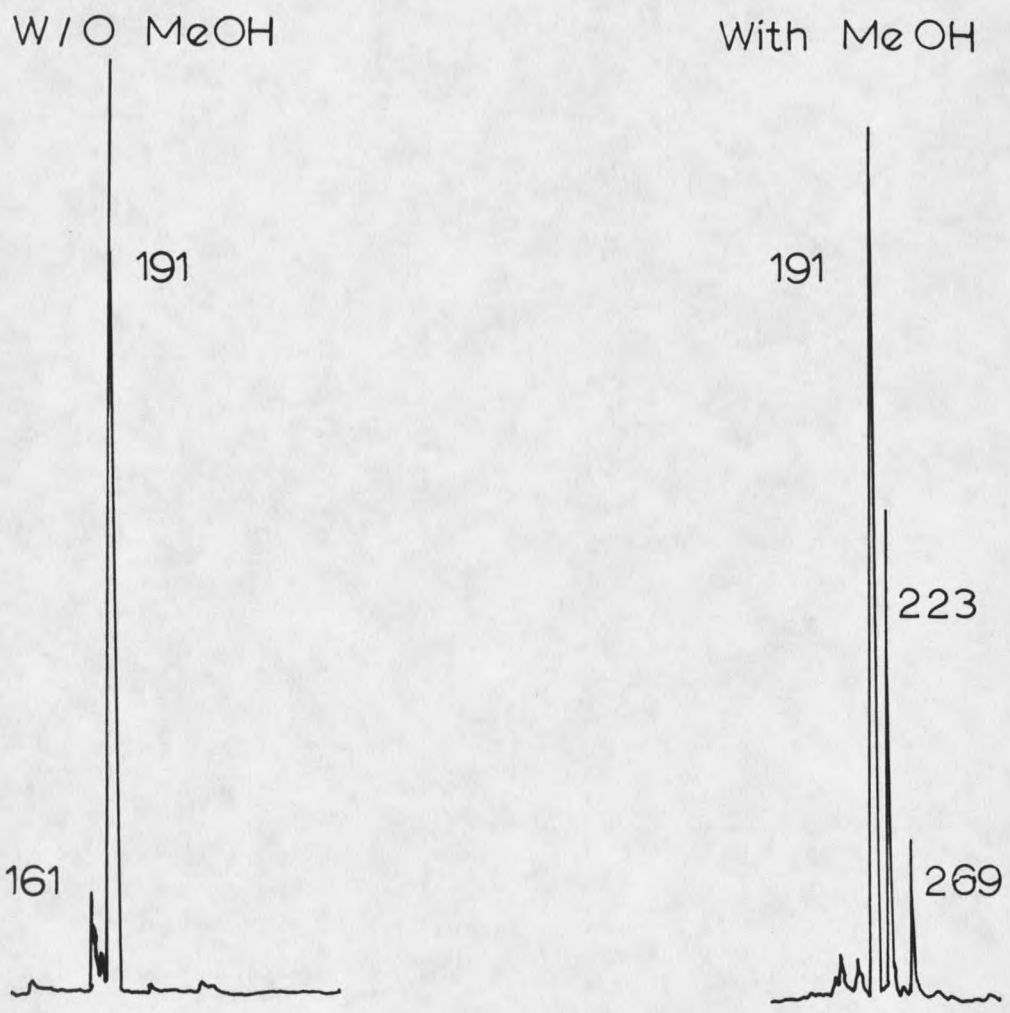

Figure 8. Ion scan of m-CF_3NB and MeOH. 191 is the molecular ion, 223 is the solvated ion, and 269 is M^- solvated by the remaining DMSO in diluter.

Figure 9. Ion scan of o-NT with and without MeOH. M^- is 137, MS^- is 169.

Figure 10. Ion scan of m-NT with and without MeOH. M^- is 137, MS^- is 169.

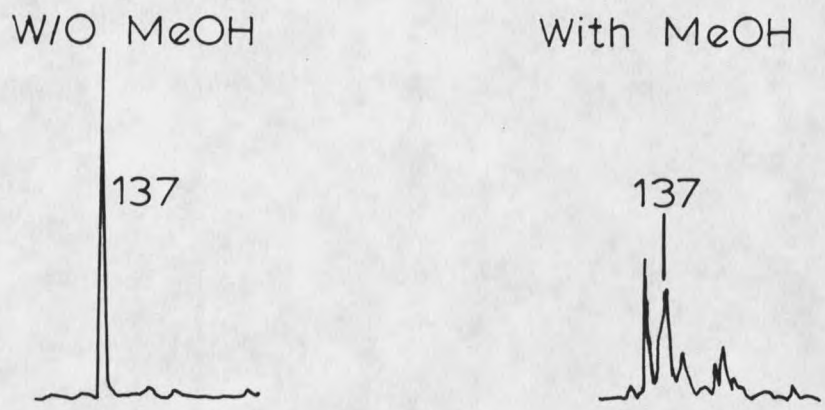

Figure 11. Ion scan of p-NT with and without MeOH. M^- is 137, MS^- is 169.

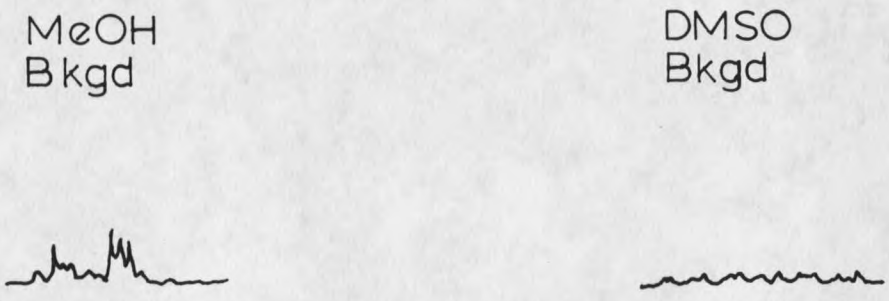

Figure 12. MeOH Background, x10, resolution 6, T_d = 170°C
DMSO Background, x10, resolution 6, T_d = 150°C.

Table 3. Ion Intensities and R Values for m-CF_3NB/0.38 torr DMSO

	INTENSITY				
MS^- (269)	11.5	10.0	5.0	2.0	1.5
M^- (191)	57.0	58.5	47.0	36.0	12.5
R (269/191)	0.202	0.171	0.106	0.056	0.120

The inequality of observed and expected values for R may be explained by aperture effects. In the region of the aperture, extreme temperature, pressure and velocity gradients exist. There is an expansion region on the exit side of the aperture where collisions can occur which may result in the dissociation of the MS^- cluster. If f is the fraction of MS^- that falls apart to M^-, and no M^- is destroyed, the observed ratio would be a function of the real ratio or the real K_f value. This does not explain the inequality of the observed ratios, however.

A possible explanation for the inequality of the observed ratios is that during the time between observing the M^- and MS^- masses, the ratio remains constant, but the intensities of M^- and MS^- change as the peak elutes from the column. Figures 13 and 14 show plots of the intensity of an ion vs. scan number, revealing that the M^- and MS^- concentrations definitely appear to change at different rates. This could be an artifact of the time it takes

to scan from M^- to MS^-. Even at the fastest scan rate on the mass spectrometer, a change of 78 mass units takes 1 to 2 seconds. During that time, the concentration of M in the source may change, altering the observed intensity of MS^-, because the concentration of M^- has changed according to the equilibrium of the electron capture reaction.

This phenomena is also observed for other compounds as shown in Tables 4 - 6. Despite these discrepancies, the preliminary data suggest that this system has promise. Comparing the average R values from Tables 4 - 6 to each other and seeing that as K_f[70] for these isomers increases, so does the average R values, suggests that the method works, but that the data measurement method may be causing the variation of R. Thus, a better method of measurement must be devised. Also, the concentration of S should be better controlled, thus the invention of the bubbler described previously.

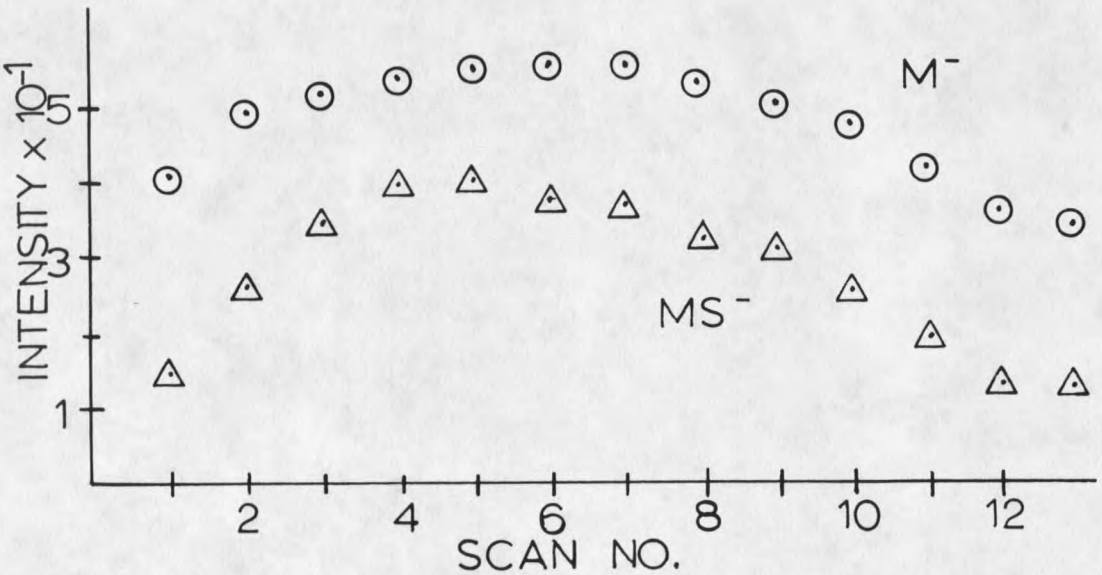

Figure 13. Intensity vs. Scan Number for m-CF_3NB/MeOH.

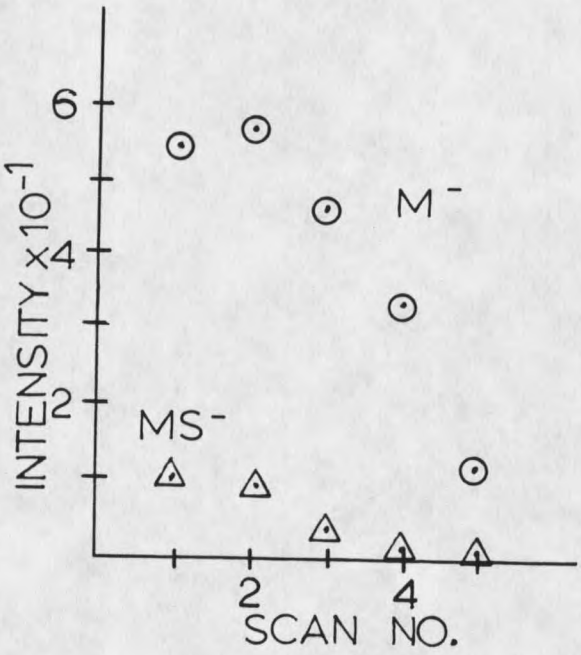

Figure 14. Intensity vs. Scan Number for m-CF_3NB/DMSO.

Table 4. Scan Number and Ratios for o-diNB/MeOH

Scan # :	1	2	3	4	5	6	7
Ratio $\frac{MS^-}{M^-}$:	0.31	0.15	0.28	0.37	0.27	0.17	0.13

Ave. R : 0.24

$K_f^{70} = 1.3 \times 10^2$ atm^{-1}

Table 5. Scan Number and Ratios for m-diNB/MeOH

Scan # :	1	2	3	4	5	6	7
Ratio $\frac{MS^-}{M^-}$:	0.32	0.36	0.36	0.30	0.18	0.24	0.18

Ave. R : 0.26

$K_f^{70} = 2.5 \times 10^2 \text{ atm}^{-1}$

Table 6. Scan Number and Ratios for p-diNB/MeOH

Scan # :	1	2	3	4	5	6	7
Ratio $\frac{MS^-}{M^-}$:	0.064	0.067	0.125	0.107	0 092	0.063	0.053

Ave. R : 0.081

$K_f^{70} = 3 \times 10^1 \text{ atm}^{-1}$

With the bubbler set-up, the concentration of S in the source is constant, if the temperature of the bubbler remains constant. There is no exponential dilution factor as with the diluter, so an experiment can be repeated at different times of the day with the same concentration of S present, and thus obtain identical results.

Since the preliminary method of measuring the ratio of $[MS^-]$ to $[M^-]$ was not reliable, a new method was devised. Instead of looking at "instantaneous" ratios from a scan, the total ratio

was looked at. This was accomplished by monitoring first one ion with a single injection of sample and then repeat the injection and monitor the other ion of interest. The areas of the peaks were then found with a planimeter, and the ratio of the areas was calculated. Figures 15 - 18 show the single ion monitor traces for the fluoronitrobenzenes and m-CF_3NB, all with DMSO as solvator. Table 7 gives the areas of the peaks and their ratios. The expected R for m-CF_3NB solvated with DMSO turns out to be 0.19, which agrees with the experimental value.

Table 7. Peak Areas and Ratios for Some Fluorinated Nitrobenzenes

Compound	A_{MS^-}	A_{M^-}	$[MS^-]/[M^-]$
o-FNB	0.16	0.24	0.67
m-FNB	0.07	0.12	0.57
p-FNB	0.13	0.17	0.79
m-CF_3NB	1.14	0.22	0.19

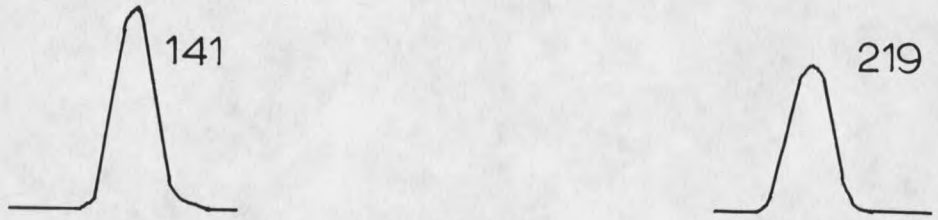

Figure 15. Single Ion Monitor of M^- (141) and MS^- (219) for o-FNB/DMSO.

Figure 16. Single Ion Monitor of M^- (141) and MS^- (219) for m-FNB/DMSO.

Figure 17. Single Ion Monitor of M^- (141) and MS^- (219) for p-FNB/DMSO.

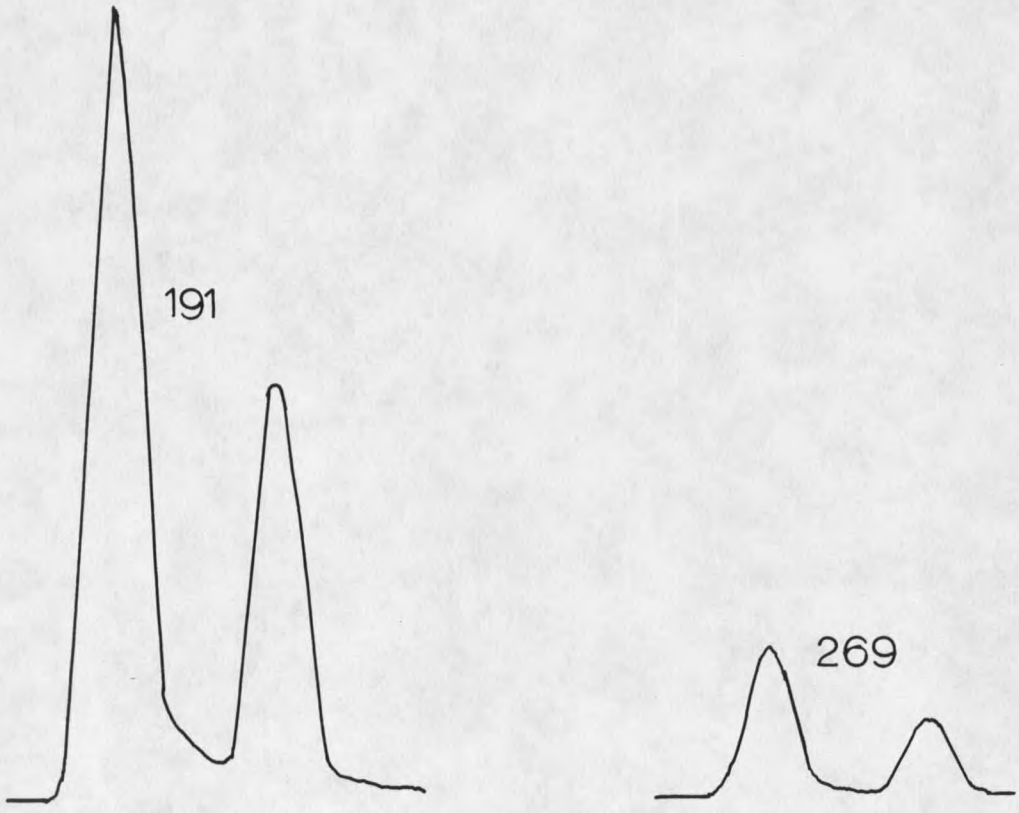

Figure 18. Single Ion Monitor of M^- (191) and MS^- (269) for m-CF_3NB/DMSO.

A better sampling mode was developed to monitor both M^- and MS^- during the same chromatographic peak. This would insure that both ions were measured under identical conditions. Details of the circuit were described previously in the experimental section. A sample of the dual ion monitor (DIM) chart record was also shown previously in Figure 5.

Since there are many variables to adjust in order to make a measurement, the optimum settings for resolution, DIM sampling speed, ion energy, concentration of analyte, and old or new bubbler, were obtained by experiment. Table 8 gives the data obtained for the system p-CNNB/DMSO for the pulse and resolution experiments. There is little effect on the ratio caused by varying the parameters of pulse speed and resolution.

Table 8. Results of Pulse and Resolution Experiments for p-CNNB/DMSO

Pulse	Resolution	Ratio of $[MS^-]/[M^-]$
A	7.0	0.097
A	6.5	0.097
A	6.0	0.097
A	5.8	0.084
A	5.5	0.100
B	6.0	0.093
C	6.0	0.095

A is 1.5 sec./pulse.
B is 0.75 sec./pulse.
C is 2 sec./pulse.

Concentration also appears to have little effect on the observed ratio of MS^-/M^-. Table 9 shows the data obtained for p-CNNB/DMSO. The predicted ratio is 0.002, which is quite different from the observed ratio of 0.13, however both concentrations gave the same ratio.

Table 9. Concentration Effect on the Ratio of $[MS^-]/[M^-]$

Concentration	Area MS^-	Area M^-	R
60 ng	0.11	0.82	0.13
12 ng	0.66	5.08	0.13

The ion energy parameter was checked at full ion energy (24V) and half ion energy (12V), using the "old " bubbler. The system used was m-CF_3NB/DMSO, because the K_f value was high, and there was significant signal for both M^- and MS^- ions. As shown in Figure 19, the full ion energy of 24 volts should be used, as less than full energy did not produce as straight a line from a plot of lnK vs. $1/T_d$.

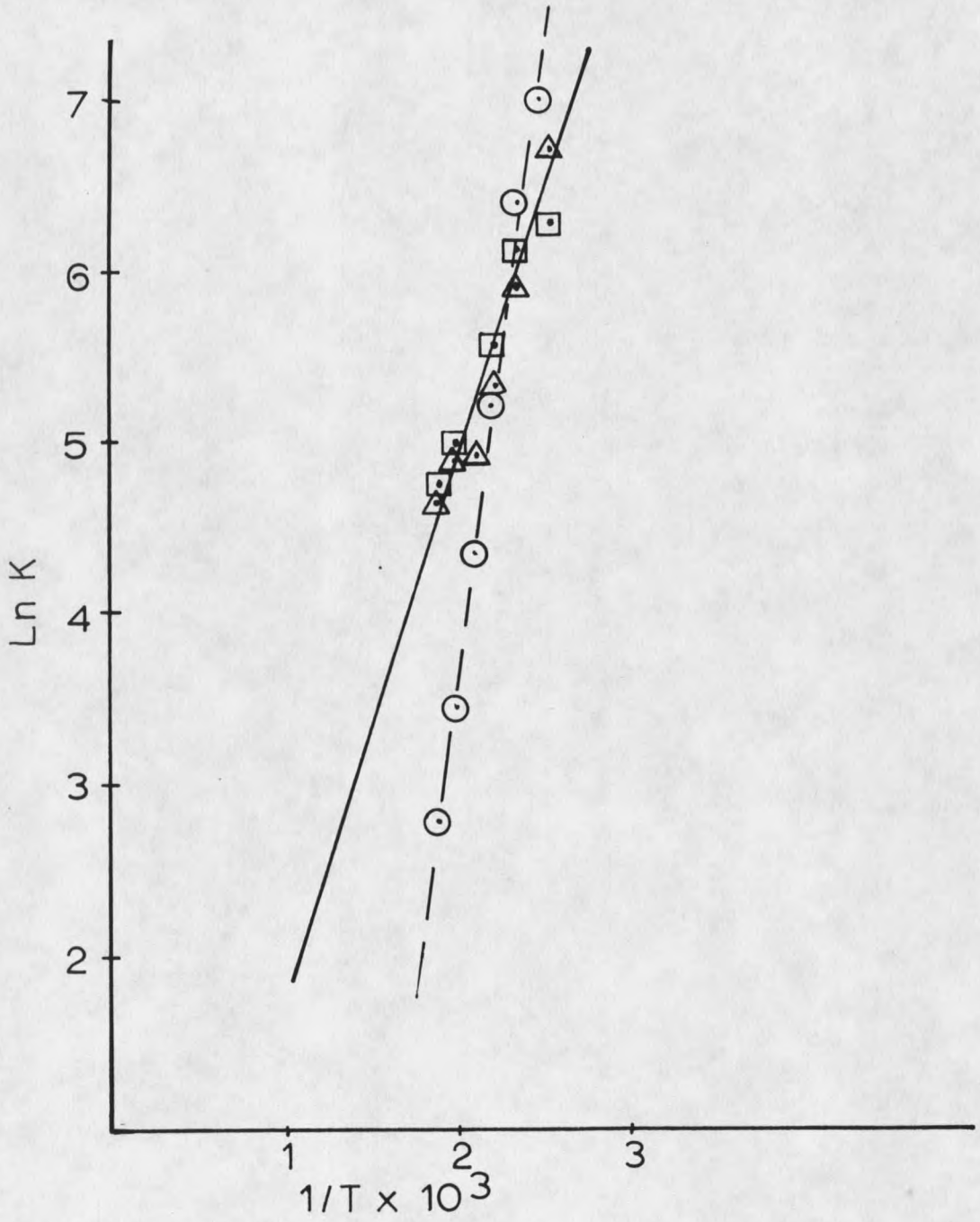

Figure 19. Ln K vs. 1/T for Various Ion Energies, and for Calculated Points from Kebarle's Data, ⊙ . 24 Volts, ⊡ , 12 Volts △ .

The two bubblers were compared by repeating the experiment with the same analyte compounds, meta- and para-nitroanisole (m and p-OCH_3NB) with DMSO. The K_f values at a source temperature of 150°C were compared against the concentration, or partial pressure, of DMSO. The partial pressure of DMSO was calculated by plotting the Merck Index values on a graph, drawing a curve, and then reading the corresponding pressures from the experimental temperatures. As can be seen in Figure 20, there is no significant difference in the K_f values obtained from the two bubblers.

The test for equilibrium in the source was accomplished by monitoring K_f^{exp} vs. [S]. If equilibrium is achieved, K_f^{exp} should be a constant value no matter what [S] is. Only the ratio MS^-/M^- should change as [S] changes. This is not the case as shown in Figure 21 for para- and meta-nitroanisole, and Figure 22 for para-cyanonitrobenzene (p-CNNB). All three compounds have the same shaped curve, so there must be some sort of relationship between K_f and [S].

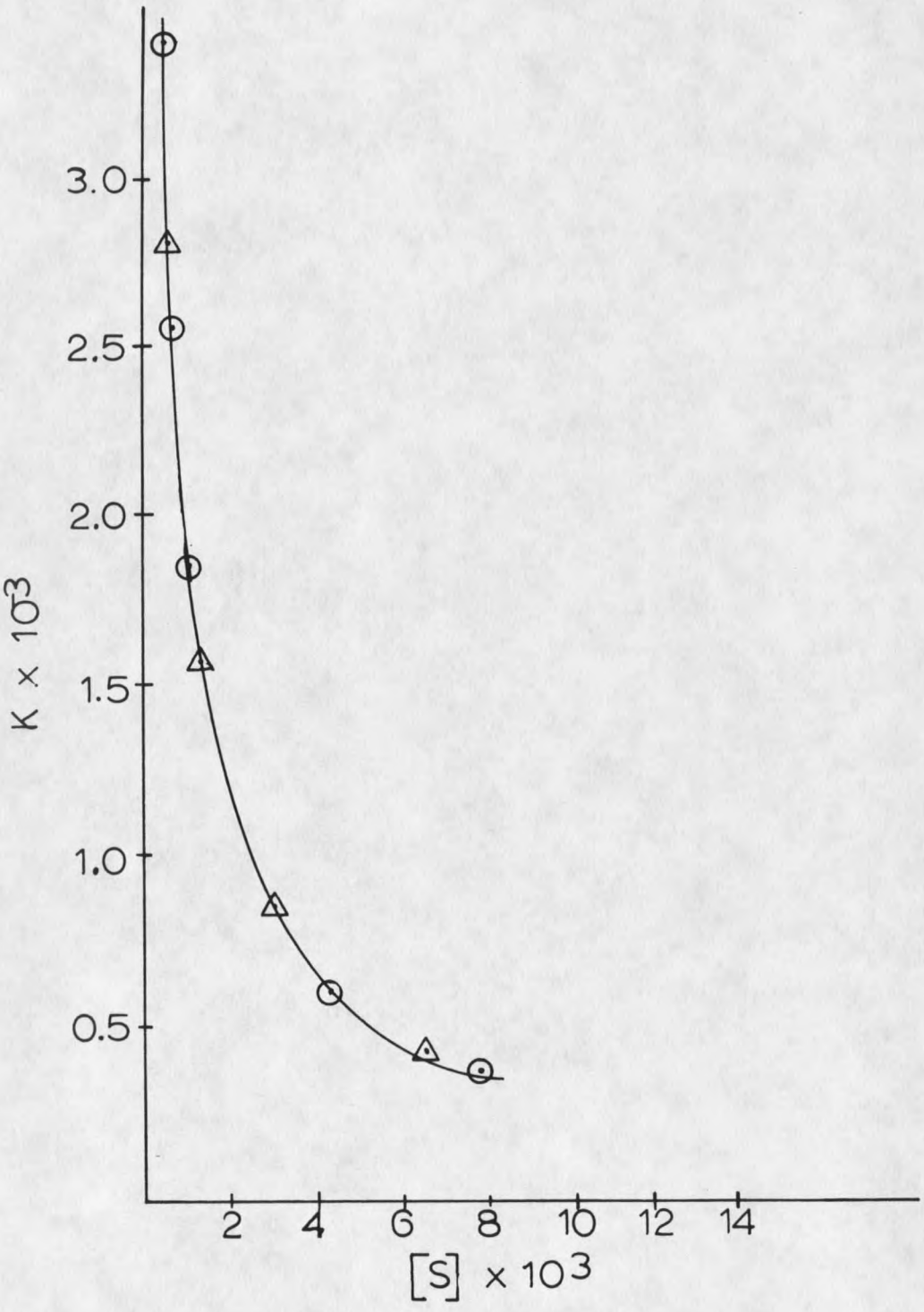

Figure 20. Comparison of K_f vs. [S] for Original ⊙ and Improved △ Bubblers. K is atm^{-1}, [S] is atm.

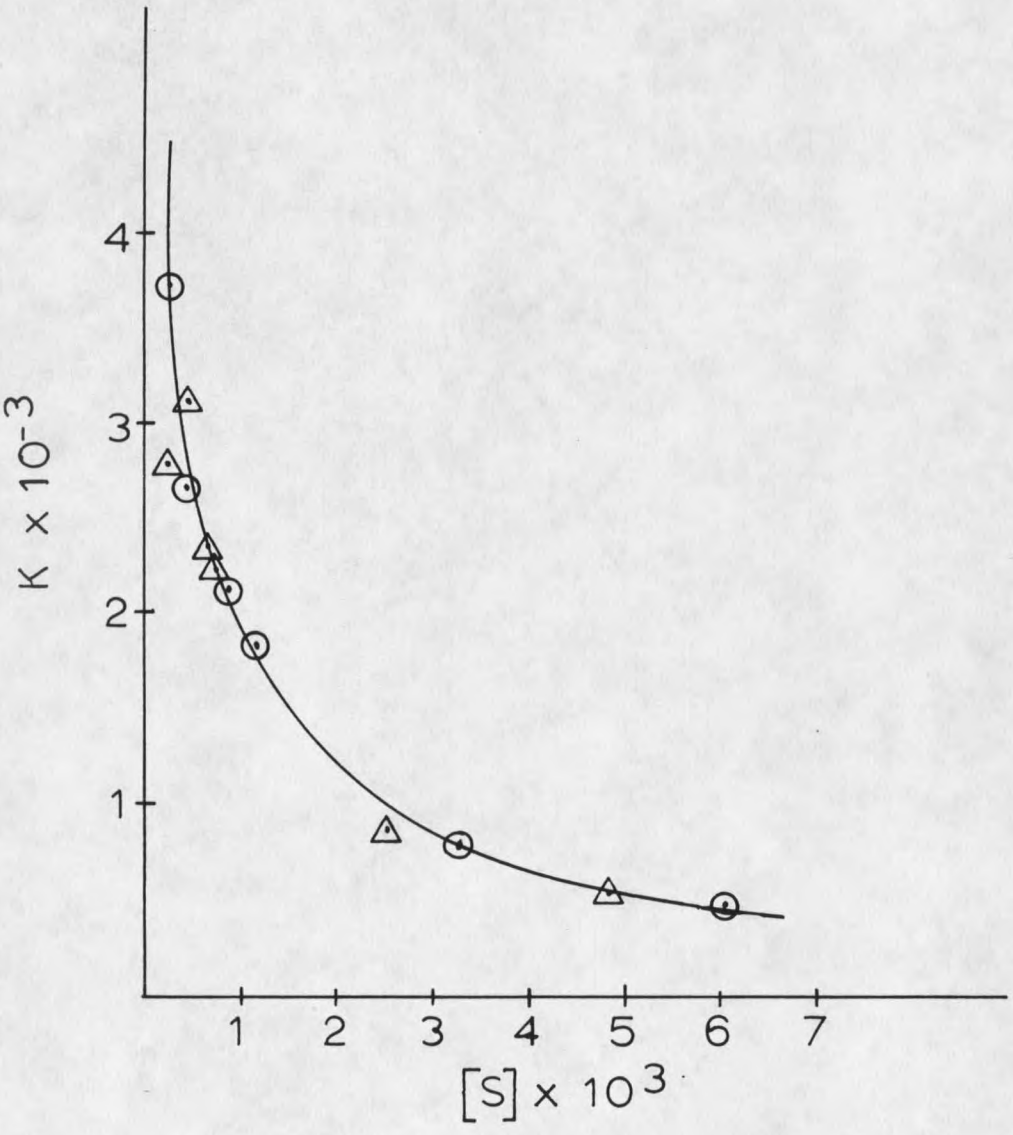

Figure 21. K_f vs. [S] for p-OCH_3NB, ⊙ , and m-OCH_3NB, △ . K is in atm^{-1}, [S] is in atm.

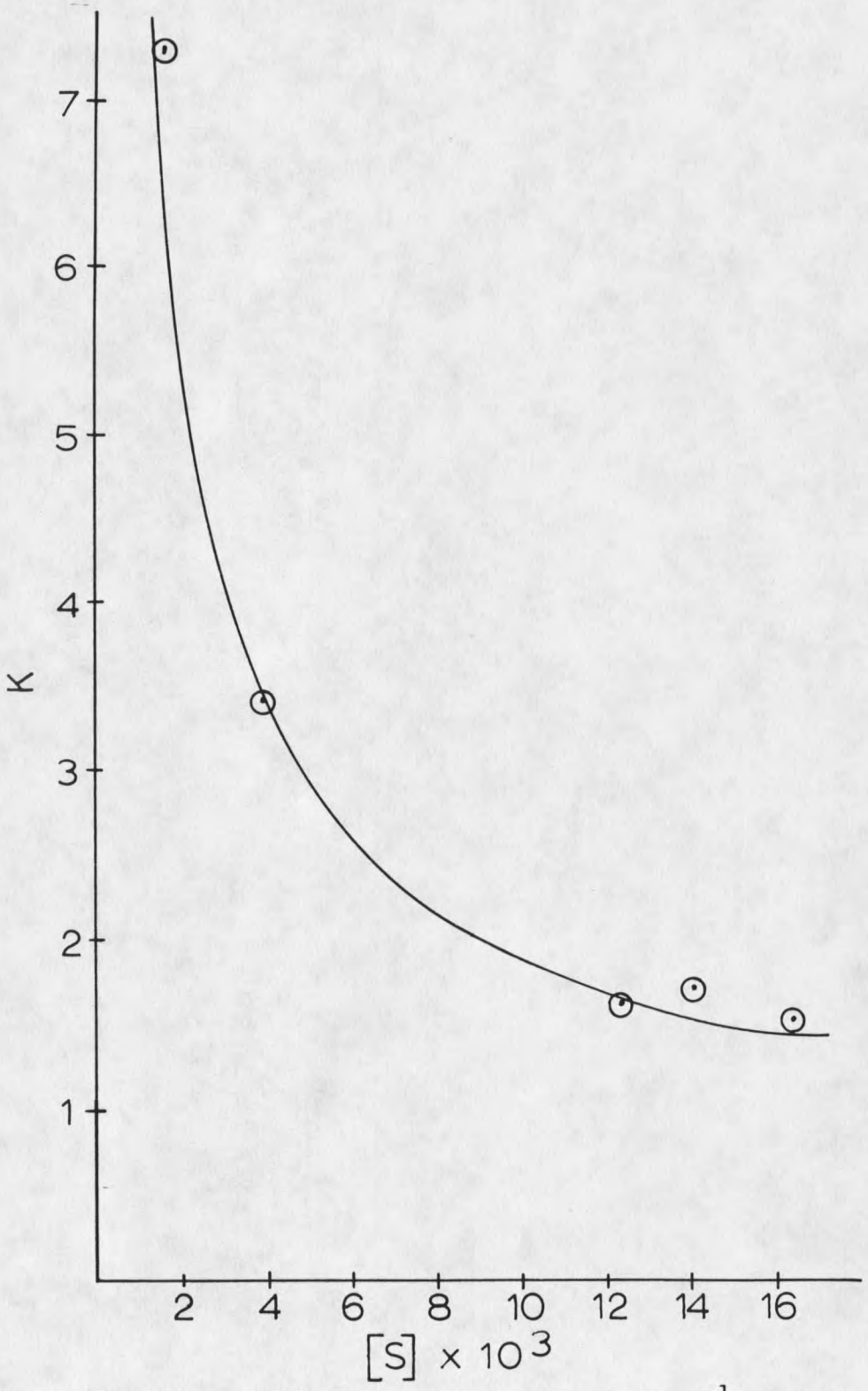

Figure 22. K_f vs. [S] for p-CNNB. K is in atm^{-1}, [S] is in atm.

One possible explanation is the aperture effect described previously. In the expansion region through which gas passes into the evacuated, mass analyzing region, collisions occur[2] that reverse the solvation process. For example:

$$MS^- + N_2 \longrightarrow M^- + S + N_2$$

This reaction would reduce the observed intensity for the ion MS^- and increase the intensity for M^- by a fraction, f. Writing this in terms of the chemical equilibria happening, assuming M^- does not dissociate:

(20) $$K_{exp} = \frac{[MS^-]_o}{[M^-]_o[S]}$$

(21) $$\frac{[MS^-]_o}{[M^-]_o} = \frac{[MS^-]_r - f[MS^-]_r}{[M^-]_r + f[MS^-]_r}$$

(22) $$K_r = \frac{[MS^-]_r}{[M^-]_r[S]}$$

(23) $$[MS^-]_r = K_r[M^-]_r[S]$$

(24) $$\frac{[MS^-]_o}{[M^-]_o} = \frac{K_r[S][M^-]_r - K_r[S][M^-]_r f}{[M^-]_r + K_r[M^-]_r[S]f}$$

(25) $$\frac{[MS^-]_o}{[M^-]_o} = \frac{K_r[S] - K_r[S]f}{1 + K_r[S]f}$$

(26) $$= K_r[S]\frac{(1 - f)}{(1 + K_r[S]f)}$$

(27) $$\frac{[MS^-]_o}{[M^-]_o[S]} = K_r\frac{(1 - f)}{(1 + K_r[S]f)}$$

(28) $$K_{exp} = K_r\frac{(1 - f)}{(1 + K_r[S]f)}$$

Using this final expression to generate a predicted plot of K_{exp} vs. [S] from appropriately chosen values for [S] and K_r, the graph in Figure 23 is obtained, which closely resembles the data

plotted earlier in Figures 21 and 22. Therefore, the expression 28 is a possible description of the aperture effect.

Unfortunately, the values for f and K_f are not easily found without a linear relationship. A rearrangement of the above equation resulted in giving a linear relationship for all of the compounds tested by this method.

$$(29) \qquad \frac{1}{K_{exp}} = [S]\frac{f}{(1 - f)} + \frac{1}{K_r(1 - f)}$$

The slope is equal to $f/(1 - f)$ and the intercept, $1/K_r(1 - f)$, enabling the calculation of f and K_r. Figures 24 to 26 show the graphs obtained from data for m-OCH_3NB, p-OCH_3NB, p-CNNB, o-FNB, m-FNB and p-FNB. Table 10 gives the pertinent values. All K_r^{calc} values are at 150°C except p-CNNB, which is at 225°C.

Table 10. Comparison of K_r^{calc} and K_f^K for Some Fluoronitrobenzenes from Equation 29

Compound	Corr. Coeff.	f	K_r^{calc}	K_f^K
m-OCH_3NB	0.997	0.27	4628	--
p-OCH_3NB	0.998	0.25	7800	3200
p-CNNB	0.984	0.78	425	0.48
o-FNB	0.989	0.08	102	--
m-FNB	1.000	0.09	33,300	97,600
p-FNB	0.990	0.09	78,500	161,000

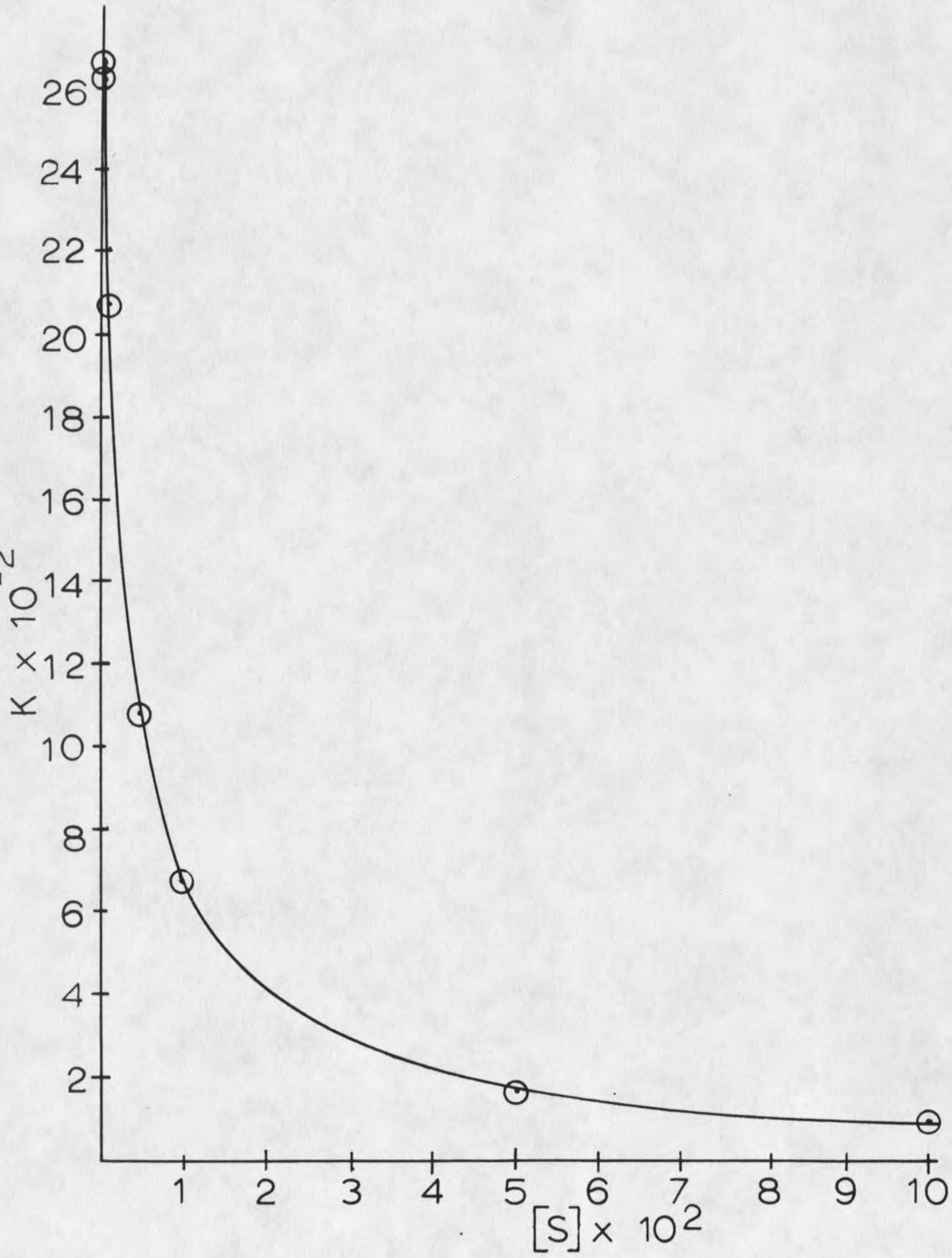

Figure 23. Generated Plot of K vs. [S] from Equation 29.

Here, K = 3000 and f = 0.10.

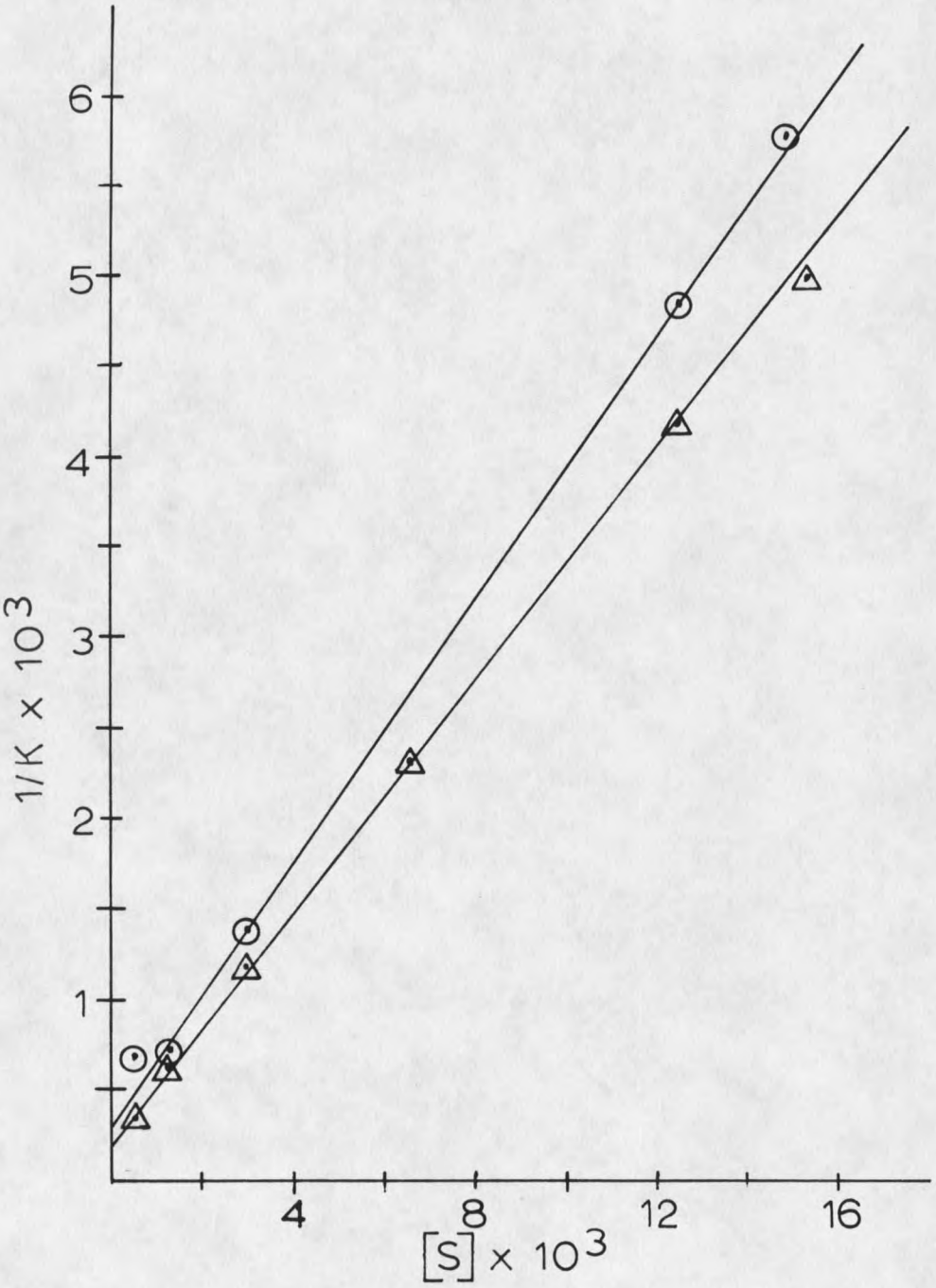

Figure 24. $1/K_{exp}$ vs. [S] for m-OCH_3NB, ⊙ and p-OCH_3NB, △ with DMSO. T_d = 150°C

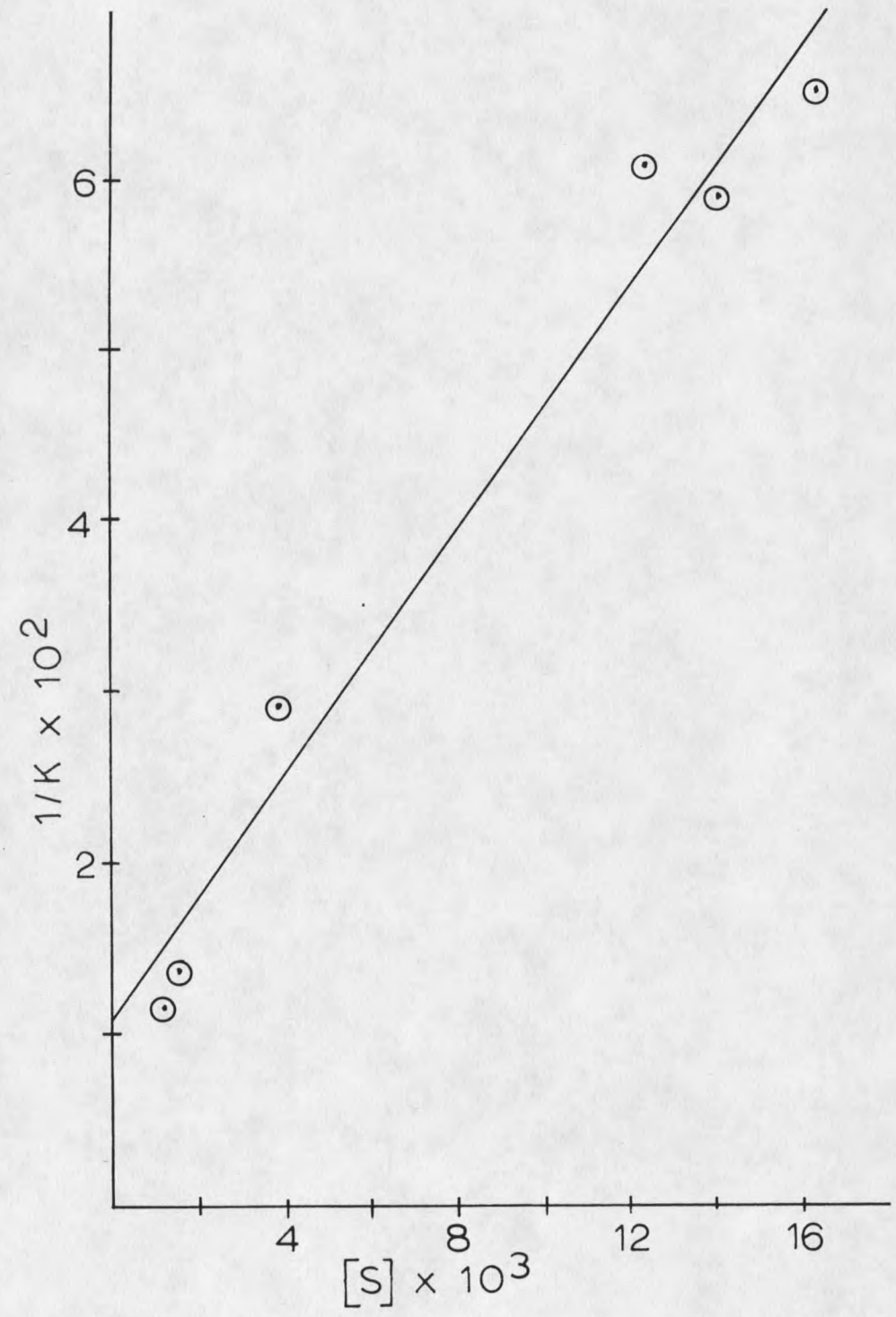

Figure 25. $1/K_{exp}$ vs. [S] for p-CNNB with DMSO. T_d = 150°C. K is in atm^{-1}, [S] is in atm.

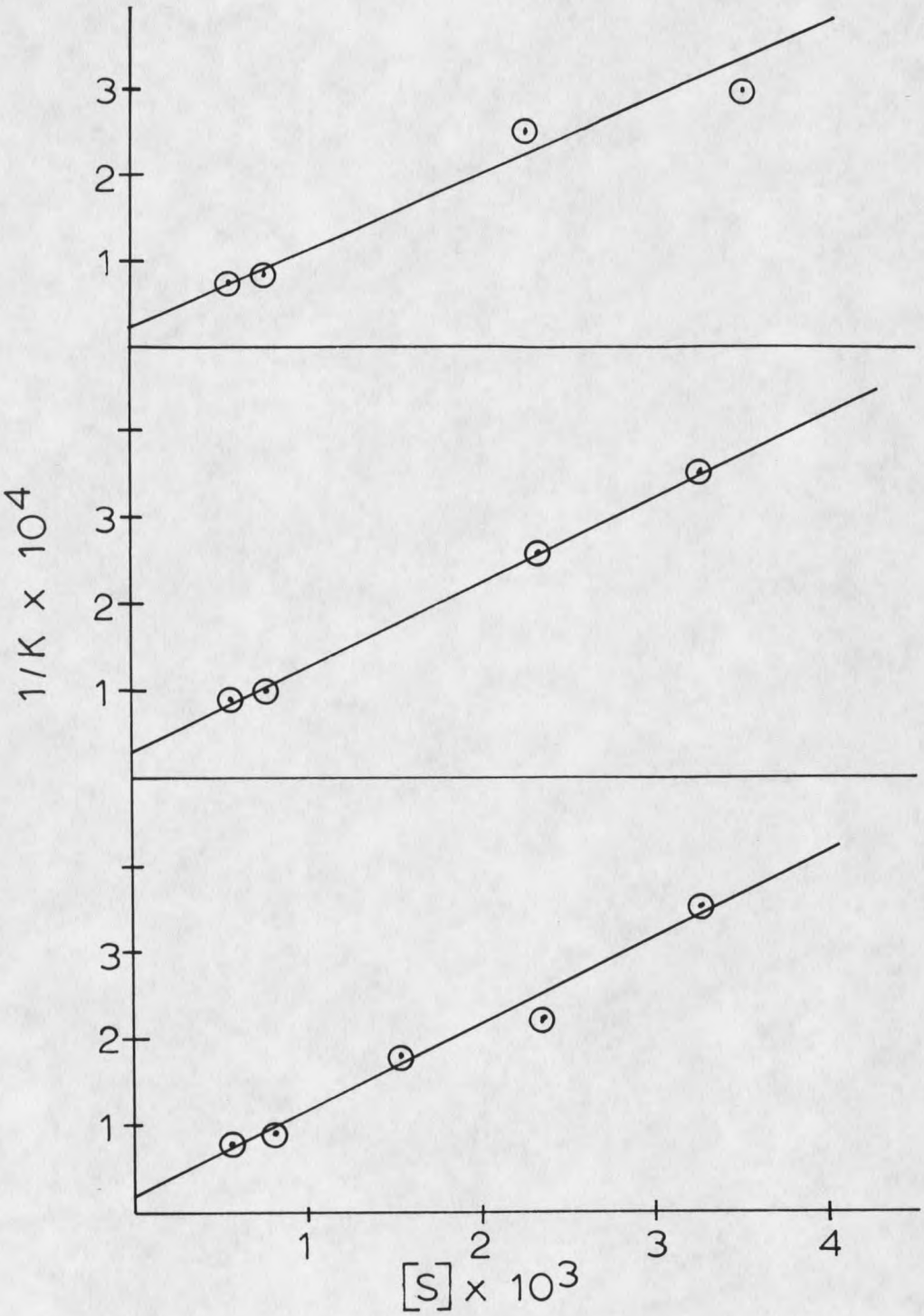

Figure 26. $1/K_{exp}$ vs. [S] for (from top to bottom) o, m, and p-FNB with DMSO. $T_d = 150^{o}C$. K in atm^{-1}, [S] in atm.

The correlation coefficient was calculated from a linear regression program from Sharp Electronics Corporation on their model EL-512 calculator. A value of 1.000 means all of the data points lie on the line. As seen from the graphs and the correlation coefficients, $1/K_f$ vs. [S] is a linear relationship for the compounds tested.

This linear relationship did not lead to the correct calculated K_f value when compared to Kebarle's, so the relationship just discussed is not perfectly expressed as

$$(23) \qquad \frac{1}{K_{exp}} = [S]\frac{f}{(1 - f)} + \frac{1}{K_r(1 - f)}$$

Other expressions were investigated before Eq. 29, searching for a linear relationship between [S] and R or K. One of these that showed promise was:

$$(30) \qquad \frac{1}{R} = \frac{1}{K_r(1 - f)}\frac{1}{[S]} + \frac{f}{(1 - f)}$$

which gave a linear relation for four out of five compounds tested. See Figures 27 to 29 and Table 11. Applying this same formula to the solvation of the FNB's by two molecules of DMSO did not result in a linear relationship, Figure 31, suggesting that the system is more complicated than this expression suggests. Also, since it did not result in a linear relationship for p-CNNB, this expression does not correctly describe the system that is being studied. Further manipulations were made to ultimately reach equation 29, resulting in linear relationships for all compounds tested.

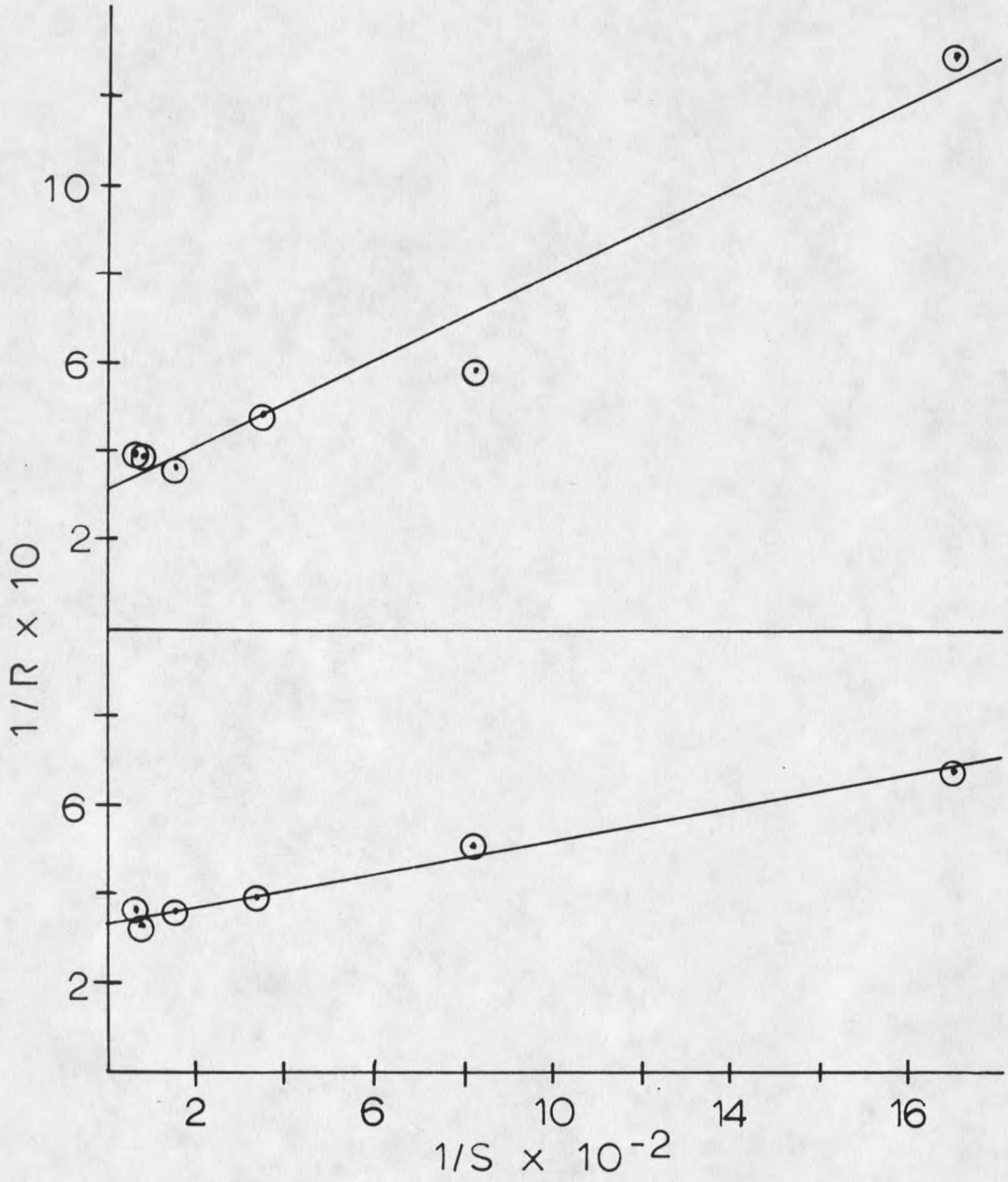

Figure 27. 1/R vs. 1/[S] for (from top to bottom) m-OCH_3NB and p-OCH_3NB with DMSO. T_d = 150°C. [S] in atm.

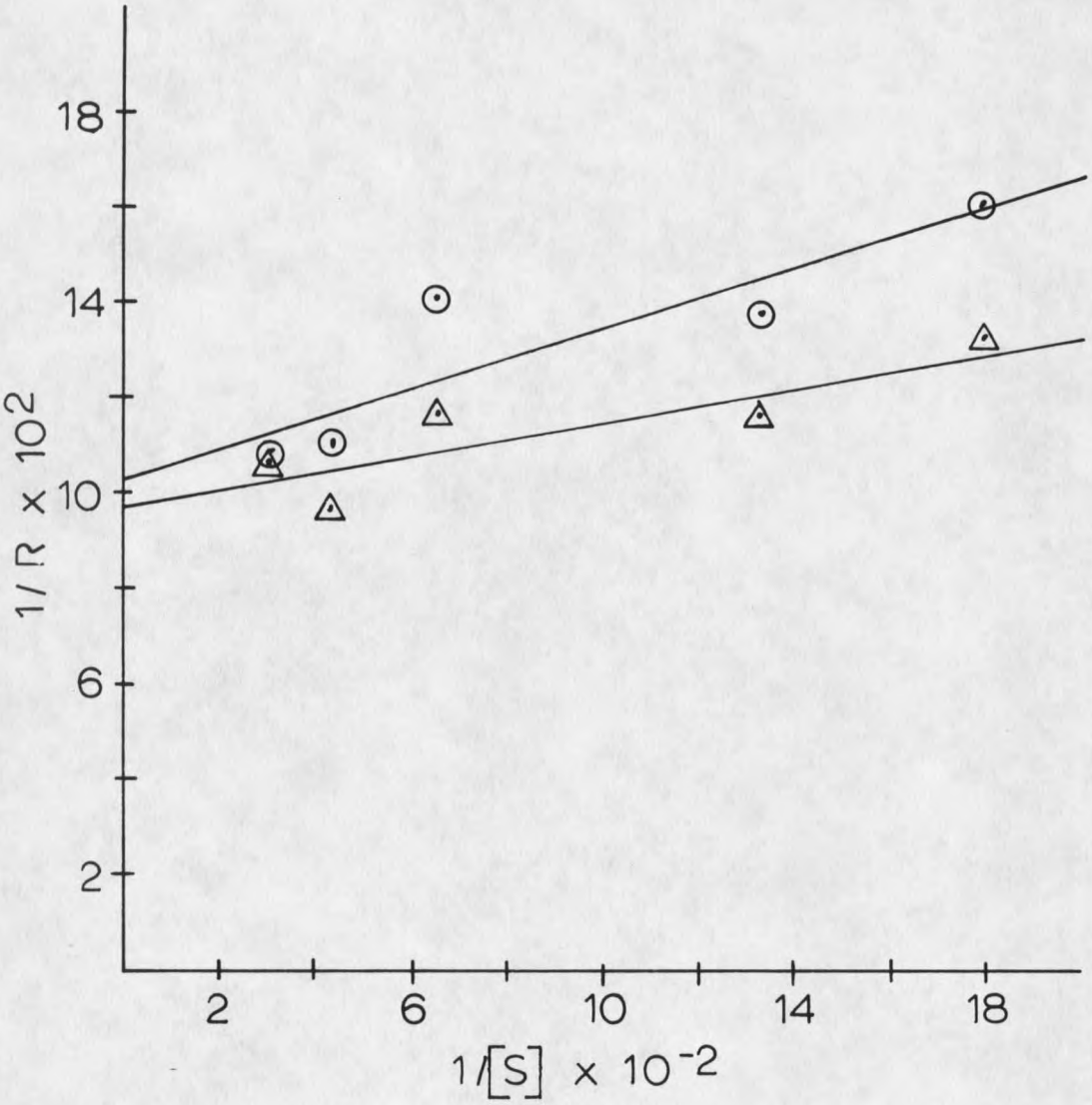

Figure 28. 1/R vs. 1/[S] for m-FNB, ⊙ and p-FNB, △ with DMSO. T_d = 70°C. [S] in atm.

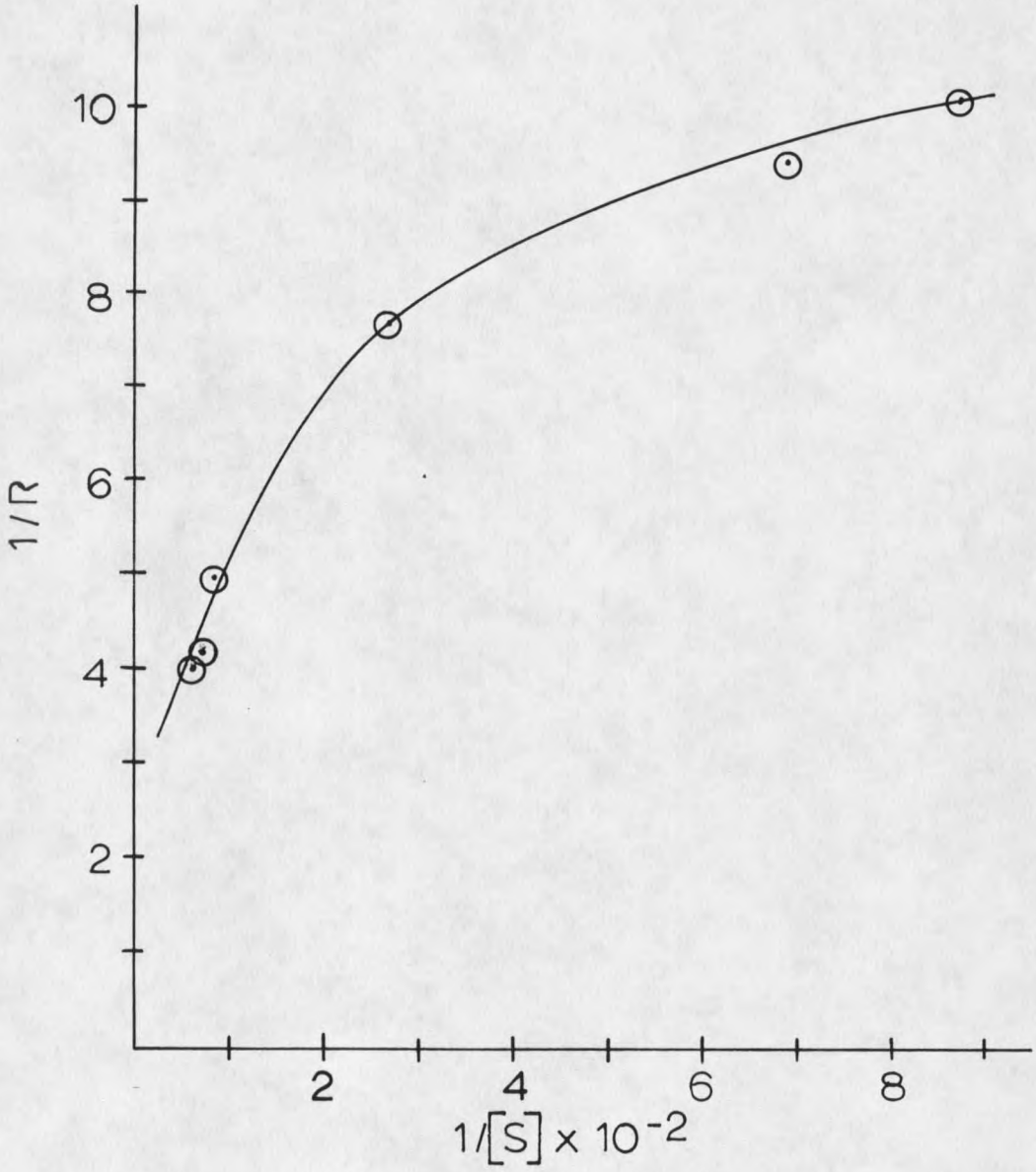

Figure 29. 1/R vs. 1/[S] for p-CNNB with DMSO.

T_d = 225°C. [S] in atm.

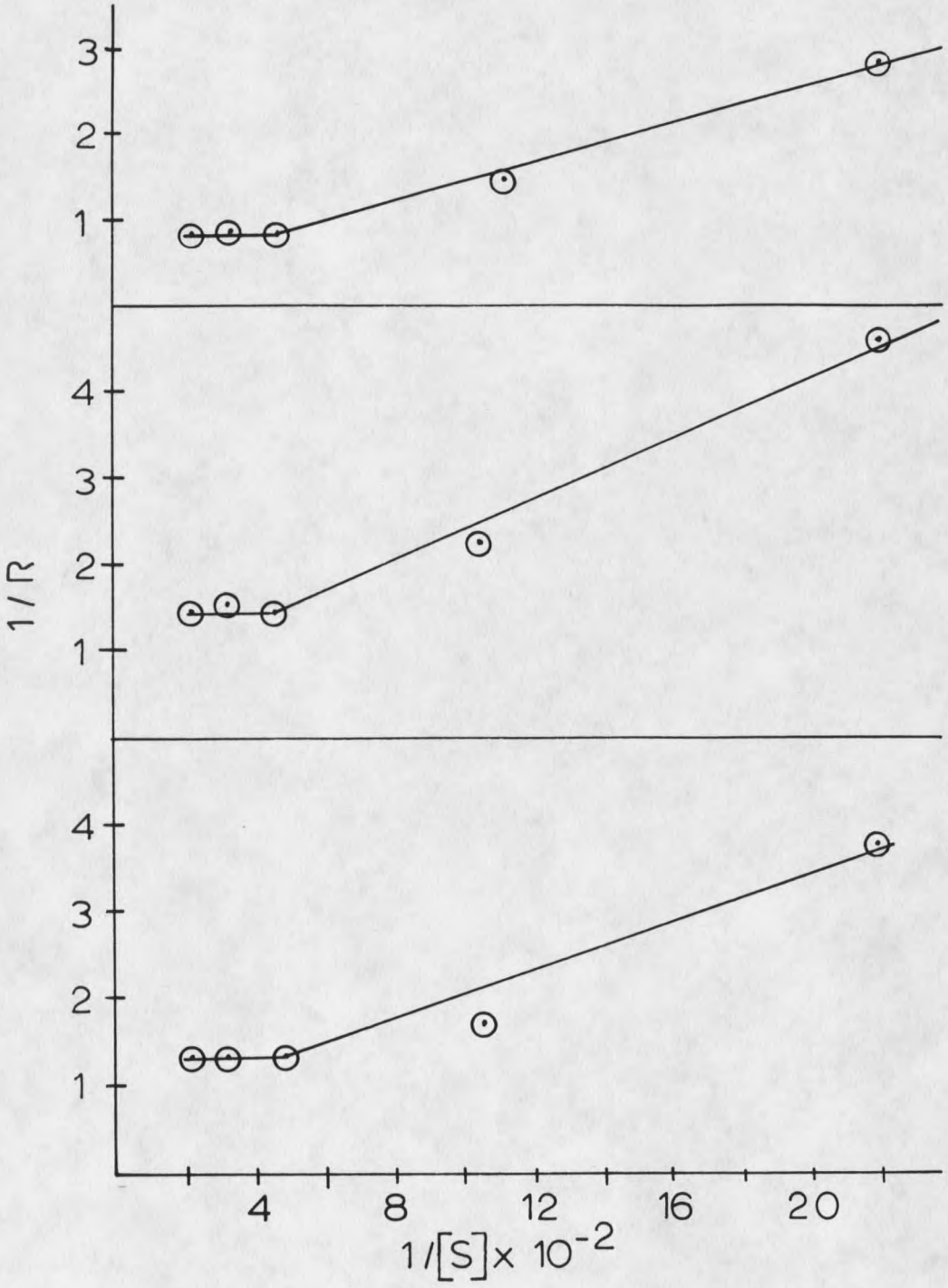

Figure 30. 1/R vs. 1/[S] for solvation of M^- by two molecules of DMSO. M (from top to bottom) is o, m, and p-FNB. [S] in atm.

Table 11. Comparison of K_f^{calc} and K_f^{K} for Some Fluorinated Nitrobenzenes from Equation 30

Compound	Slope	Intercept	f	K_f	K_f^K
m-OCH_3NB	5.3×10^{-4}	0.31	0.24	2700	--
p-OCH_3NB	1.8×10^{-4}	0.34	0.254	7285	3196
m-FNB	3.5×10^{-5}	0.10	0.093	34,800	97,600
p-FNB	1.9×10^{-5}	0.10	0.088	60,000	161,000

The best expression was equation 29, correlating $1/K_f$ and [S]. This is not yet the accurate expression, as the experimental K_f values calculated do not appear correct. However, the reference K_f values may be in question to some degree as Kebarle admits to errors in his ΔH and ΔS values which were used to calculate the reference K_f's. More compounds should be tested against this theory to verify it and to derive any other possible additions or variations to it.

SUMMARY

According to the theoretical calculations done in the Chemical Dynamics section, thermodynamic equilibrium is achieved in the API source. The preliminary data of K_f vs. [S] however, seems to show that the API signals do not reflect this equilibrium. This conflict of theory and data may be resolved by closely examining what happens between the source and the detector. Leaving the source, the ions and neutrals must pass through an aperture into the evacuated region containing the lenses, quadrupoles and detector. As the ions, etc. pass through the aperture, there are extreme temperature, pressure, and velocity gradients. In this chaotic zone, collisions can occur which could break apart a solvated ion, MS^- to M^-. Other things may happen, such as removing the electron from M^-, making it a neutral and unobservable. Also, the temperature change may alter the equilibrium, affecting the observed intensity of the MS^- and M^- ions. One expression that was examined was equation 28:

$$(28) \qquad K_{exp} = K_r \frac{(1 - f)}{(1 + K_r[S]f)}$$

This equation generated a curve that resembled the data plotted for K_f vs. [S]. This suggests that the theory expressed above (eq. 28) closely describes why the expected horizontal line for the graph K_f vs. [S] is not observed. Since curved lines do not afford much information, and do not clearly define a

relationship, other variations of equation 28 were tried, hoping for a linear relation of some sort between K_f, or R, and [S].

One variation discussed, 1/R vs. 1/[S] (equation 30), resulted in straight lines for four compounds (m-OCH_3NB, p-OCH_3NB, m-FNB and p-FNB) but curves for the rest, including the double solvation of M^- by two molecules of DMSO. This, then, was not especially useful. The relationship that gave the closest apparent description of the aperture effects was equation:

$$(29) \qquad \frac{1}{K_{exp}} = [S]\frac{f}{(1 - f)} + \frac{1}{K_r(1 - f)}$$

which gave linear plots for every compound that had the data available to use the above relationship. Table 11 shows that r, the linear correlation coefficient, for all compounds was above or equal to 0.984. Four of the six compounds had values above 0.990. An r of 1.000 means all of the data points are on the line. So the agreement of data to the best possible line is very good for all of the compounds. This supports the theory of equation 29, that the aperture causes a variation in the observed equilibrium by causing a fractional loss, f, of MS^- and an increase of M^- to (M^- + fMS^-).

Also, the value f is not constant and varies from compound to compound. The magnitude of f does seem to be tied to the K_f^K value, as seen in Table 11. For the four K_f^K values available, it appears that as K_f^K increases, f decreases. This makes sense because the larger the K_f^K value, the more stable the solvated

ion would be. This stronger stability would reduce the amount lost due to collisions, thus lowering the value of f.

In general, the solvation equilibrium method of isomer distinction shows considerable promise. In the preliminary experiments, the ratio of MS^-/M^- increased as the K_f value increased (Tables 4 - 6) for a given series of isomers. So far, the analytical applications of this method are limited. The aperture effects need to be more closely studied. The final relationship, equation 29, still does not give the expected K_f values of Kebarle. Nevertheless, the linear relationships obtained are encouraging. Additional work is required to further clarify the relationship between the reactions occurring in the source and the observed signals.

REFERENCES CITED

1. Chowdhury, S.K., E.P. Grimsrud, and P. Kebarle. "Bonding of Charge Delocalized Anions to Protic and Dipolar Aprotic Solvent Molecules," J. Phys. Chem., In Press, 1987.

2. Kolaitis, L. and D.M. Lubman. Anal. Chem. 58, (1986).

3. Harrison, Alex G. "Chemical Ionization Mass Spectrometry," CRC Press Inc., Boca Raton, FA.,1983.

4. McKeown, M. and M.W. Siegel, Am. Lab., Nov., 1975.

5. Sears, L.J., J.A. Cambell, and E.P. Grimsrud. Biomed. and Environ. Mass Spec., accepted Jan. 1987.

6. Smith, David and Nigel Adams in, "Physics on Ion-Ion and Electron-Ion Collisions," ed. by F. Brouillard and J.W. McGowan, Plenum Press, New York, 1983.

7. Knighton, W.B. and E.P Grimsrud, J. Chromatogr., 288,(1984).